

# Politecnico di Torino

Master's degree in Environmental and Land Engineering
"Industrial Environmental Sustainability"

A.A. 2024/2025

Graduation session: November 2025

Managed Aquifer Recharge Monitoring:
The Case Study of the SeTe Alcotra Project

Advisors:
Prof. Casasso Alessandro
Co-advisors:

Taramasso Maria Adele Gallia Lorenzo **Candidate:**Dalè William

#### **ABSTRACT**

Climate change is continuously challenging water supply worldwide, enhancing the pressure on groundwater resources. The international community is working to address this issue, by developing new solutions for sustainable water management strategies. Among various adaptation measures, Managed Aquifer Recharge (MAR) represent an effective natural-based solution to enhance groundwater storage and mitigate drought effects. This thesis evaluates the feasibility and hydrological impacts of two MAR infrastructures located in the Province of Cuneo, in the Piedmont Region (Northwestern Italy), within the framework of the European SeTe-Alcotra project. The systems, located in the municipalities of Beinette and Tetti Pesio, were designed to increase the aquifer recharge outside irrigation periods, when water availability is higher, thus improving water supply stability throughout the year.

The objective of the study is to evaluate the volume of water infiltrated through the MAR systems, and to assess their influence on the underlying aquifer, separating it from the effects of natural precipitation. A combination of field monitoring data, spatial analysis with QGIS, and temporal correlation between hydrological variables was applied to evaluate infiltration rates, delineate drainage basins, and analyse precipitation—groundwater interactions.

At the Beinette site, during the study period from April to July 2025, the MAR system infiltrated a total water volume of  $140,773 \, m^3$ , with an average flowrate of  $50.13 \, m^3 h^{-1}$ . The precipitation study, individuated three pluviometric stations representing rainfall over the Beinette basin, used to estimate the mean precipitation. A temporal lag of  $10 \, days$  between precipitation and aquifer response was observed. Although MAR infiltration appeared to contribute to the rise in groundwater levels, the limited monitoring period did not allow for a clear quantification of the correlation between MAR infiltration and aquifer response.

At the Tetti Pesio site, infiltration occurred only during two short events (29 April and 8 May 2025), each lasting a few hours, which did not allow for a reliable estimation of infiltrated volume or detectable aquifer response. Nevertheless, the monitoring network provided an essential framework for future analyses and establishes baseline hydrogeological conditions for the area. Thirteen pluviometric station were used to estimate the mean precipitation over the basin. Similarly, in Tetti Pesio basin, the hydrological study estimated a **10** *days* temporal lag between precipitation and aquifer response.

The main limitations of the study are related to the short monitoring period and the limited operational activity of the MAR infrastructures. However, the results confirm the MAR potential as effective, natural-based solutions for groundwater resource enhancement. Future

developments should focus on extending monitoring period, improving data resolution, and analysing recharge behaviour during dry season to better isolate MAR influence on the aquifer.

# **Table of Contents**

1 INT	INTRODUCTION			
2 CLI	MATE CHANGE: IMPACTS ON WATER CYCLE AND THE ROLE	OF		
MAR TE	CHNOLOGIES	3		
2.1	Overview of Climate Change: Origins, Effects and Mitigation Politicies	3		
2.1.1	Origins of the climate change			
2.1.2	Effects			
2.1.3	International political framework	5		
2.2	Climate Change Effects on Water Cycle	5		
2.2.1	Precipitation			
2.2.2	Evapotranspiration	6		
2.2.3	Cryosphere	6		
2.2.4	Streamflow	7		
2.2.5	Floods and droughts	7		
2.2.6	Groundwater	7		
3 STA	TE OF THE ART OF MANAGED AQUIFER RECHARGE: HISTOR	RY,		
	IQUES AND APPLICATIONS	•		
3.1.1	Historical evolution of MAR	9		
3.2	MAR Objectives	10		
3.2.1	Maximize natural storage capacity	10		
3.2.2	Sustainable management of groundwater resources	10		
3.2.3	Prevention of saltwater intrusion	11		
3.2.4	Water quality management	11		
3.2.5	Sustain environmental surface water flows	11		
3.2.6	Prevention of land subsidence	11		
3.3	MAR Classification	12		
3.3.1	Well, shaft and borehole recharge	13		
3.3.2	Spreading methods	14		
3.3.3	Induced bank filtration	15		
3.3.4	In-channel modifications	15		
3.3.5	Rainwater and runoff harvesting	16		
3.4	Implementation of MAR Worldwide	17		
3.4.1	Securing water supply to Windhoek, Namibia	17		
3.4.2	Soil aquifer treatment to protect coastal ecosystem in Agon-Coutainville, France	17		
3.4.3	A coastal plain groundwater reservoir in Shandong, China	18		
3.5	Clogging: A Key Operational Challenge in MAR Systems	18		

	3.5.1	Physical clogging	18
	3.5.2	Chemical clogging	19
	3.5.3	Biological clogging	19
	3.5.4	Mechanical clogging	19
4	LEC	GISLATIVE FRAMEWORK	21
	4.1	International Overview	21
	4.2	The Italian Framework	22
5	SeT	e-ALCOTRA PROJECT	24
	5.1	Geological Framework	24
	5.1.1	Beinette geological framework	25
	5.1.2	Tetti Pesio geological framework	26
	5.2	Hydrogeological Framework	27
	5.2.1	Beinette hydrogeological framework	28
	5.2.2	Tetti Pesio hydrogeological framework	29
	5.3	Design and Functioning of the MAR Structures	30
	5.3.1	Beinette recharge trench	30
	5.3.2	Tetti Pesio recharge trench	31
	5.4	Monitoring System of the Project	32
6	ME'	THODOLOGY	36
	6.1	Assessment of Infiltrated Volume	36
	6.1.1	Beinette recharge trench	36
	6.1.2	Tetti Pesio recharge trench	40
	6.2	Assessment of the Precipitation Contributing to Aquifer Recharges	43
	6.2.1	Basin delineation with QGIS	44
	6.2.2	Thiessen Polygons for the basin rainfall precipitation	44
		Assessment of the Temporal Lag between Precipitation and Water Table Lev	vels46
	6.4	Assessment of the MAR Influence on the Underlying Aquifer	46
7	RES	SULTS	47
	7.1	Beinette	47
	7.1.1	Volume of water infiltrated	
	7.1.2	Precipitation study	49
	7.1.3	MAR infiltration and groundwater relation	
	7.2	Tetti Pesio	55

9	REF	ERENCES	64	
8 CONCLUSION			62	
	7.2.3	Groundwater levels	60	
	7.2.2	Precipitation study	56	
	7.2.1	Volume of water infiltrated	55	

## 1 INTRODUCTION

The increasing pressure on water resources, driven by climate change and population growth, has made the development of sustainable water management strategies a global priority. Several studies have highlighted the effects of climate change on the hydrological cycle, reducing groundwater storage and enhancing the problem of water scarcity worldwide. All components of the hydrological system are affected, including precipitation, evapotranspiration, cryosphere, streamflow, and finally groundwater.

Groundwater is one of the main freshwater resources for drinking water supply, agricultural production and industrial activities, especially in areas where surface water availability is limited or highly variable. For this reason, its sustainable use and protection have become one of the principal goals of the international community.

In fact, in the 2030 Agenda for Sustainable Development of the United Nations, the sixth Sustainable Development Goal expresses the importance of an efficient use of water resources, supported by transboundary cooperation. At the European level, water resources are protected by two Directives, the Water Framework Directive, which provides a general outline for the protection of all water bodies, and the complementary Groundwater Directive, which constitutes the basis for the groundwater protection in the European Union. These Directives are transposed at the national level in Italy through the Testo Unico Ambientale, which, among other objectives, regulates groundwater protection and discharges. The entire legislation framework identifies Managed Aquifer Recharge (MAR) as a strategic tool to counteract the effects of climate change on groundwater resources.

MAR refers to the intentional replenishment of groundwater aquifers in order to enable future reuse or to provide environmental benefits. The first MAR systems date back 200 BC, but only with the advancement of hydraulic theory of the last centuries they have reached a high technical level and become globally widespread. Although this technology can serve numerous objectives, such as preventing saltwater intrusion, sustaining surface water flows, or preventing land subsidence, its main purpose is to maximize the natural storage capacity of the aquifers. The diffusion of MAR systems is due to their natural-based approach and low level of engineering. Furthermore, MAR technologies present several design and construction variants, making them adaptable to a wide range of scenarios.

This study focuses on the feasibility of two MAR infrastructures installed in the Piedmont Region, specifically in the municipalities of Beinette and Tetti Pesio, near the city of Cuneo. Their construction is part of the SeTe-Alcotra project, a European transboundary program between

Italy and France with the purpose of mitigating the adverse effects of extreme events such as droughts and floods. The area of study has been affected by droughts in recent years, in fact, in 2022 Piedmont experienced the worst water scarcity in the last 75 years. The main objective of the planned MAR systems is to increase the aquifer storage outside of the irrigation season by exploiting the water coming from the Alps, thereby ensuring a more stable water supply throughout the year.

To evaluate the two MAR infrastructure, this study aims to estimate the infiltrated water volume through the recharge trenches and to investigate its effects on the underlying aquifer. In order to isolate the MAR influence from the meteorological precipitation, a precipitation study was conducted. This analysis was also useful to establish the temporal lag between the infiltration and aquifer response. To achieve these objectives, a combination of field monitoring data, spatial analysis with QGIS, and temporal correlation between hydrological variables was used.

The thesis is structured in eight chapters:

- ➤ Chapter 2 provides an overview on climate change and its impacts on the hydrological cycle, with a particular focus on the effects of groundwater resources.
- ➤ Chapter 3 present the state of art of MAR, including its historical evolution, main objectives, typologies, and global applications, as well as operational challenges such as clogging.
- ➤ Chapter 4 outlines the legislative framework regulating MAR infrastructure at global, European and Italian scales.
- ➤ Chapter 5 introduces the SeTe-Alcotra project and describes the geological and hydrogeological backgrounds of Tetti Pesio and Beinette sites, along with the description of the monitoring network and technical descriptions of their functioning.
- ➤ Chapter 6 details the adopted methodology for assessing infiltrated volume, precipitation contribution, temporal lag, and MAR influence on the aquifer.
- ➤ Chapter 7 presents and discusses the results obtained from the analysis.
- Chapter 8 presents the conclusions derived from this study

Overall, this research contributes to a better understanding of MAR performance in the Piedmont region and supports the integration of artificial recharge into groundwater management strategies under changing climate.

# 2 CLIMATE CHANGE: IMPACTS ON WATER CYCLE AND THE ROLE OF MAR TECHNOLOGIES

Climate change has significantly contributed to water scarcity issues in recent decades. MAR technologies have emerged as strategic tools to address or mitigate these challenges by improving the availability and sustainable management of water resources.

This chapter aims to provide a framework of climate change, with a particular focus on its impacts on the water cycle.

#### 2.1 Overview of Climate Change: Origins, Effects and Mitigation Politicies

Before addressing the phenomenon of climate change, it is necessary to define the concept of climate and distinguish it from weather. Weather refers to the atmospheric conditions, such as temperature, cloudiness, humidity, precipitation and wind, observed at a specific location and time over short periods. In contrast, climate is defined as the long-term average of weather patterns that characterize a specific region, typically calculated over periods longer than thirty years [1], [2].

Climate change refers to a persistent alteration of this long-term weather patterns averages [3]. Therefore, it is crucial to analyse trends over extended periods, in order to distinguish climate change from climate variability. In fact, the latter refers to fluctuations of the prevailing climate that occur over different temporal and spatial scales, while climate change refers to a change in the climate state lasting several decades or more [1].

#### 2.1.1 Origins of the climate change

Climate is a complex system, characterized by continuous interactions among the land surface, hydrosphere, biosphere, and atmosphere, which plays the most significant role. The climate system derives its energy from the Sun, and the Earth's radiative balance can be altered by changes in the amount of incoming shortwave solar radiation, surface albedo, and outgoing longwave emissions [1].

This delicate equilibrium can be destabilized by both natural phenomena and human activities. Earth's climate has always undergone natural fluctuations over time. For instance, cycles of solar activity and changes in the Earth's orbit around the Sun influence the amount of incoming solar radiation, thereby affecting the radiative balance [1].

However, since the 19<sup>th</sup> century, human activities have become the primary driver of global climate change [2]. With the advent of industrialization, the emission of greenhouse gases (GHGs) into the atmosphere began to increase significantly, thereby accelerating global warming. GHGs are those gases responsible for the greenhouse effect, the process by which the

atmosphere is able absorb and re-emit outgoing longwave radiation emitted by the Earth's surface, effectively trapping heat within the atmosphere. However, this natural balance has been increasingly damaged by human activities. The combustion of fossil fuels for electricity generation and industrial processes, alongside population growth, land-use changes and urban expansion, has led to a rapid rise in atmospheric GHG concentrations. As a result, the greenhouse effect has been amplified, driving modern climate change [1].

#### 2.1.2 Effects

Climate change has clear environmental impacts, closely linked to a wide range of socio-economic consequences. The most evident manifestation is the increase in global average temperature. According to the European Union's Earth observation program Copernicus, global temperatures in 2024 were recorded to be 1.6 °C above pre-industrial levels [4]. As a result, a wide range of environmental and health-related effects are increasingly evident worldwide.

Ecosystems face significant stress from the increase in extreme weather events, including floods and extreme drought, causing loss of human and animal life, destruction of agricultural lands, and reductions in biodiversity. Moreover, the rainfall patterns are undergoing substantial alterations, with some regions becoming increasingly arid and others experiencing more frequent and heavier precipitation. Climate models estimate that for every 1 °C rise in average global temperature, average global precipitation increase by approximately 2 %. Importantly, climate change not only alters the quantity of rainfall, but also its intensity and distribution, leading to more frequent and extreme precipitation events [5].

Sea levels have been rising over the past decades because of the combination of melting ice sheets and thermal expansion of seawater due to warming. This trend is contributing to coastal land loss and the displacement of millions of people, as many of the world's most densely populated cities, such as Lagos, Calcutta or Shanghai, are located near sea level [5], [6].

These environmental changes have profound socioeconomic repercussions. National economies are predicted to lose up to 8 % of gross domestic product. Such losses are largely driven by declines in agricultural productivity, forestry, fisheries, and water availability. As a result of these mounting issues, an increasing number of people are being forced to migrate. In some cases, this mass displacement can lead to social and political instability, leading to violent conflicts [1], [5]. A more detailed discussion on the effects of climate change on the water cycle is provided in the Section 2.2.

#### 2.1.3 International political framework

To address the challenges posed by climate change, governments worldwide have reached and ratified various agreements and protocols. Since the environment has no borders, transboundary cooperation is fundamental, and the effort must be collective. However, international law faces a major problem, the sovereignty of individual states, which make it difficult to enforce sanctions and obligations. Consequently, the implementation of international agreements heavily relies on the political will of individual nations [7].

Human activities were firstly recognized as a driver of climate change in the United Nations Framework Convention on Climate Change (UNFCCC), adopted in 1992 during the first Earth Summit in Rio. The main objective of the Convention was to stabilize the GHG emissions at a level that would prevent dangerous anthropogenic interference with the climate system [8], [9]. The UNFCCC led to the Kyoto Protocol, adopted in 1997, which introduced internationally binding emission reduction targets during the commitment period 2008-2012 [9], [10].

In 2015, the Paris Agreement replaced the Kyoto Protocol. The principal goal of this Agreement was to limit the increase in global average temperature to well below 2 °C above pre-industrial levels, while pursuing efforts to limit the rise to 1.5 °C [9], [11].

This international framework led in Europe to the European Green Deal, presented by the European Commission on 11 December 2019. The Green Deal represents a growth strategy acting on a wide range of sectors, aimed to guiding the European Union (EU) towards achieving climate neutrality by 2050. Importantly, the transition must be fair and inclusive, ensuring social equity, which is deeply challenged by climate change itself [12], [13].

#### 2.2 Climate Change Effects on Water Cycle

The water cycle has been significantly altered by climate change and global warming. Rising global temperatures have resulted in higher atmospheric moisture, primarily due to enhanced evaporation. As a result, although the average global precipitation has increased, this change is not uniformly distributed, leading to unprecedented conditions for hundreds of millions of people. Other components of the water cycle have also been affected. The frequency and the intensity of extreme events, such as floods and droughts, have increased, resulting in severe impacts upon environment, economies and social well-being. Additionally, the cryosphere has undergone substantial changes, with a marked reduction in the glacier coverage and snow extent. These phenomena, along with the environmental degradation, population growth and urbanization, are exerting increasing pressure on water resources and their management strategies worldwide [14], [15].

This section presents the main alterations to the global water, according to the Sixth Assessment Report of IPCC (AR6), published on 6 August 2021.

#### 2.2.1 Precipitation

Annual mean precipitation is increasing in numerous regions across the world, while only a limited number of areas are experiencing a decrease. Climate change is intensifying the contrast between wet season and dry season, especially in tropical areas. It is contributing to increase precipitation in northern high latitude regions, while causing drier summers in several mid-latitude and subtropical regions, including Mediterranean basins, southwestern Australia, southwestern South America, South Africa and western North America. Furthermore, the frequency of heavy precipitation events is rising across most land regions. Consequently, a substantial portion of the global population is now experiencing precipitation patterns that are significantly different from historical ones. According to AR6, nearly 500 million people are living in regions with unusually wet conditions, while over 160 million are exposed to unusual dry conditions [14].

These new precipitation patterns lead to difficulties in water management, especially since aquifers recharge heavily relies on precipitation derived water.

#### 2.2.2 Evapotranspiration

Recent studies indicate that global evapotranspiration has increased significantly since the early 1980s. This trend is driven by two primary factors, growing atmospheric demand for water and vegetation greening, which refers to the intensified activity of vegetation, mainly attributed to the higher atmospheric CO<sub>2</sub> concentration. Elevated CO<sub>2</sub> levels accelerate photosynthesis, which consequently results in higher transpiration rates. Calculations suggest that between the 1980s to the 2010s, evapotranspiration has increased by up to 10 mm/year in North America and northern Eurasia. Even greater increases have been observed in other regions including as Brazil, western central Africa, southern India, southern China and northern Australia. Conversely, decrease of 10 mm/year are experienced in parts of Amazonia and Central Africa, highlighting that non-uniform nature of this global trend [14].

The modification of global evapotranspiration has an important impact on water management. In fact, higher evapotranspiration means lower groundwater recharge, since soil moisture and infiltration are reduced.

#### 2.2.3 Cryosphere

In most regions of the world, there has been a general decrease of glaciers and permafrost extent, along with an increase of their average temperature. The Northern Hemisphere is the most

affected by this trend. Between 1981 and 2018, the snow mass decreased at an approximate rate of 5 Gt/year. This trend alters runoff seasonality, thereby affecting water supply infrastructures, particularly in basins that rely mainly on spring glaciers melt, affecting various sectors, including agriculture [14].

#### 2.2.4 Streamflow

While the global average streamflow has not undergone significant modifications, regional trends in annual streamflow have followed changes in precipitation, evaporation and temperature, which, according to AR6, are driven by the anthropogenic climate change. This situation resembles that of precipitation, creating unfamiliar conditions that people are increasingly forced to adapt to [14].

Even in this case, changes in streamflow have increased water supply stress, since surface streams and groundwater are interconnected, with aquifers recharged by water infiltrating from streamflow.

#### 2.2.5 Floods and droughts

Over the past decades, the frequency and severity of floods and droughts have increased globally, resulting in widespread damages to both natural and human systems. Floods have not a uniform pattern worldwide, as they strongly depend on characteristics of the catchment where they occur. This is due to the complex relationship between precipitation and flood generation. However, AR6 confirms that anthropogenic climate change has increased the probability of extreme precipitation event, which in turn has led to an increased frequency and magnitude of river floods in many regions. Similarly, droughts have become more frequent and intense worldwide.

These events cause significant stress on water supply, since they increase the irregularity and unpredictability of aquifers recharge [14].

#### 2.2.6 Groundwater

In most regions of the world, a general decline of groundwater storage has been experienced, particularly since the early 2000s. This trend is mainly driven by aquifer overexploitation, especially for agricultural irrigation. Groundwater recharge is directly influenced by the other components of the hydrologic cycle, which, as previously discussed, are being significantly altered by climate change. As a result, groundwater dynamics are increasingly affected. For example, in cold regions, where the recharge depends largely on snow accumulation and gradual snowmelt, the earlier onset of melting and the increasing proportion of rainfall instead of snowfall have led to reduced spring recharge. Moreover, since the recharge process is strongly linked to

precipitation patterns, which are becoming more irregular and extreme, groundwater recharge is becoming increasingly episodic and less predictable [14].

In this complex framework, MAR technologies align with climate change mitigation and adaptation strategies, representing strategic tools for the sustainable management of water resources. They offer a proper solution to counteract the impacts of climate change. By enhancing groundwater recharge, these techniques create a natural buffer that ensures water availability even under hydrological stress, thereby contributing to the long-term resilience of water system in both agricultural sectors and in urban environments.

# 3 STATE OF THE ART OF MANAGED AQUIFER RECHARGE: HISTORY, TECHNIQUES AND APPLICATIONS

Aquifers are permeable geological formations that allow water storage. They are commonly recharged by natural processes, such as water infiltration from lakes and rivers or precipitation percolating through the soil. However, various human activities can also promote recharge, which are classified in three categories:

- Unintentional recharge: occurs due to human activities not directly related to the aquifer and without specific planning. Examples include the removal of deep-rooted vegetation or land clearing.
- Unmanaged recharge: occurs through the construction of structures such as wells and sumps, primary aimed at water disposal without recovery or reuse.
- Managed recharge: occurs in a controlled and managed way through specifically designed recharge structures [16].

Managed aquifer recharge (MAR) refers to the intentional replenishment of groundwater aquifers in order to enable future reuse or to provide environmental benefits [16], [17]. MAR systems are nature-based solution, since they rely on natural infiltration and subsurface storage, and represent a low-engineered approach to water supply management [18], [19]. Moreover, compared to traditional dams and reservoirs, they have lower environmental impacts, simpler implementation, and require less maintenance [20].

In recent years, MAR techniques have been increasingly used to maintain, improve and preserve stressed aquifers [21]. The primary goal of MAR is to address the growing variability in water availability and manage the temporal mismatch between local water demand and supply [17]. This is achieved by storing excess water underground during periods characterized by low consumption or when water resources are abundant [18] to reuse it later in time when demand is higher is natural availability is lower.

MAR is widely implemented in arid and semi-arid regions, where groundwater resources are often over-extracted or affected by salinity [20]. Additionally, in urban areas, it is possible to use treated wastewater in order to exploit it as a water resource and to minimize any adverse effects deriving from their disposal [16].

#### 3.1.1 Historical evolution of MAR

The concept of MAR dates back millennia and has evolved alongside advances in hydraulic science and societal needs. The first known MAR prototypes can be traced back to the Warring

States period in China, circa 221 BC. At this early stage, the technology consisted of digging channels to facilitate water infiltration and raise groundwater levels, primarily for irrigation purposes. MAR saw little improvement until the 19<sup>th</sup> century, when industrialization and population growth led to an increased demand for water. Additionally, hydraulic theory experienced notable development, thanks to the studies of physicists such as Henry Darcy and Jules Dupuit. Systems mainly consisted of riverbank filtration and infiltration ponds for storm runoff. Subsequently, a further phase of MAR development began after World War II, as water quality and quantity became a priority for post-war reconstruction and rising urbanization. Since the 1990s, MAR has been widely applied worldwide to address water shortages and protect the environment and ecosystems [18].

#### 3.2 MAR Objectives

MAR technologies have a broad range of potential applications. The following section offers a concise description of the principal use cases.

#### 3.2.1 Maximize natural storage capacity

Storing water underground is crucial in climatic regions characterized by a marked distinction between wet and dry seasons, as it allows for a reliable and adequate water supply throughout the year. It is also highly relevant in arid regions where scarce rainfall events must be fully exploited for effective water storage. One of the key factors to consider in the application of MAR is the storage capacity of the target aquifer, which is needed to quantify the volume of water that can be stored underground. Long-term underground water storage is known as "water banking", and it has been integrated into the water management policies of several countries, such as Spain and the United States of America. Compared to surface storage, underground water storage offers several advantages, including reduced land area requirements, the possibility of locating storage systems closer to end users, and lower risks of contamination, algae growth or evaporation losses [22].

#### 3.2.2 Sustainable management of groundwater resources

MAR systems can be used to ensure the proper management of groundwater resources, aiming to promote the sustainable use of aquifers and guarantee a continuous and adequate water supply. In areas with high water demand, such as urban centres, excessive groundwater extraction may easily lead to aquifer overexploitation, which can cause various problems, including saltwater intrusion. Overexploitation is becoming increasingly widespread due to population growth and the effects of climate change. Furthermore, poor groundwater management can negatively impact social equity, since a reduced water availability creates inequality and increases poverty for those

who lose access to their water resources. It is therefore important to integrate MAR systems into a sustainable management framework that consider all components of groundwater balance [23].

#### 3.2.3 Prevention of saltwater intrusion

Saltwater intrusion is a subsurface phenomenon in which seawater spreads into freshwater aquifers, potentially contaminating drinking water supplies. It primarily affects coastal areas, where it can occur naturally due to the hydraulic connection between groundwater and seawater. The phenomenon can be increased by the overexploitation of coastal aquifers, which are often the main source of water in these regions. Excessive groundwater extraction reduces the freshwater pressure, thereby allowing saltwater to infiltrate. To prevent or mitigate saltwater intrusion, MAR technologies can be implemented to inject surplus freshwater into the coastal aquifers, creating a hydraulic barrier against salinization [24].

#### 3.2.4 Water quality management

Besides storing water, MAR systems can also aim to improve water quality, especially in cases involving treated wastewater infiltration. During the infiltration, the soil acts as natural filter, degrading nutrients and other organic contaminants along the water pathway. This process is more effective when the infiltration occurs in the unsaturated zone. The factors influencing water quality improvements include the source water quality, the MAR system design, the mixing with natural groundwater, the operational conditions and the site's hydrogeological characteristics [25].

#### 3.2.5 Sustain environmental surface water flows

There is a strong connection between groundwater and surface water, and their interaction can result in either groundwater discharging into streams or stream water percolating into aquifers. The overexploitation of groundwater may lower the water table, thereby reducing baseflow contributions to streams and increasing stream water infiltration into the subsurface. This imbalance leads to a decrease in streamflow, with negative impacts on ecosystems, water quality, and overall water availability. MAR techniques can be implemented to raise the water table and mitigate this phenomenon [26].

#### 3.2.6 Prevention of land subsidence

Land subsidence is one of the major consequences of groundwater overexploitation. It is induced by the reduction of the aquifer level, that leads to the compression of aquifer sediments and aquitards. Land subsidence can have several negative impacts, such as reduced water quality, damage to buildings, increased flood risk, and loss of aquifer storage. This phenomenon can be address with MAR systems, by restoring groundwater levels through water infiltration [27].

#### 3.3 MAR Classification

Based on the site-specific hydrogeological condition and on the purpose of the project, several MAR methods can be used to recharge the aquifers. They can be divided into five groups [17]:

- ➤ Well, shaft and borehole recharge
- Spreading methods
- > Induced bank filtration
- > In-channel modifications
- Rainwater and runoff harvesting

The first three categories mainly involve techniques aimed at promoting water infiltration, while the last two primarily focus on intercepting water [28]. The following paragraphs describe each group in more detail.

Table 1 provides an overview of the main MAR techniques discussed in this thesis.

Table 1. Managed Aquifer Recharge (MAR) classification system including five core methods and corresponding specific MAR methods.

	Main MAR Methods	Specific MAR Methods
	Well, shaft and borehole recharge	Aquifer Storage and Recovery (ASR), Aquifer Storage, Transport, and Recovery (ASTR)
Techniques aimed at promoting water infiltration	Spreading methods Soil Aquifer Treatment (SAT), Infiltration pond	
	Induced bank filtration	River/lake bank infiltration, Dune filtration
Techniques aimed at intercepting	In-channel modifications	Subsurface dams, Sand dams
water	Rainwater and runoff harvesting	Rooftop rainwater harvesting

Beyond MAR systems, aquifer recharge can be achieved through off-season irrigation and surface storage. Off-season irrigation involves the distribution of excess water to available fields or its retention within irrigation channels during the non-irrigation period, thereby enabling infiltration and percolation into the subsurface [29].

On the other hand, surface reservoirs are widely used but present several drawbacks, including high evaporation losses, extensive land requirements, sediment accumulation, potential structural failure, and vulnerability to contamination [17]. Moreover, dams usually require large distribution systems and treatment plants, especially in arid areas, where they can be affected by the growth of blue-green algae, which produce toxins [20].

#### 3.3.1 Well, shaft and borehole recharge

These MAR methods are widely used where the aquifer lies at great depth and is capped by a low-permeability or impermeable layer [18]. They consist of recharge through wells, shaft and boreholes utilizing gravitational recharge [28]. Among these techniques are Aquifer Storage and Recovery (ASR) and Aquifer Storage, Transport, and Recovery (ASTR). ASR uses a single well that serves for both recharge and extraction of water. A deep well directly connects the injection point to the aquifer to bypass the aquitard [30]. It is primarily used for water storage for potable use as well as irrigation. On the other hand, ASTR involves constructing separate wells for injection and the recovery, representing a refined version of ASR [18]. Aquifers are not inert systems but behave like biogeochemical reactors, a property exploited by ASTR for water treatment, especially for the removal of pathogens and micropollutants, by increasing the water residence time. In both cases, high water quality is required in order to avoid well clogging [16], and because water is directly injected into the aquifer [30].

In Figure 1, schematic representations of ASR and ASTR techniques are presented.

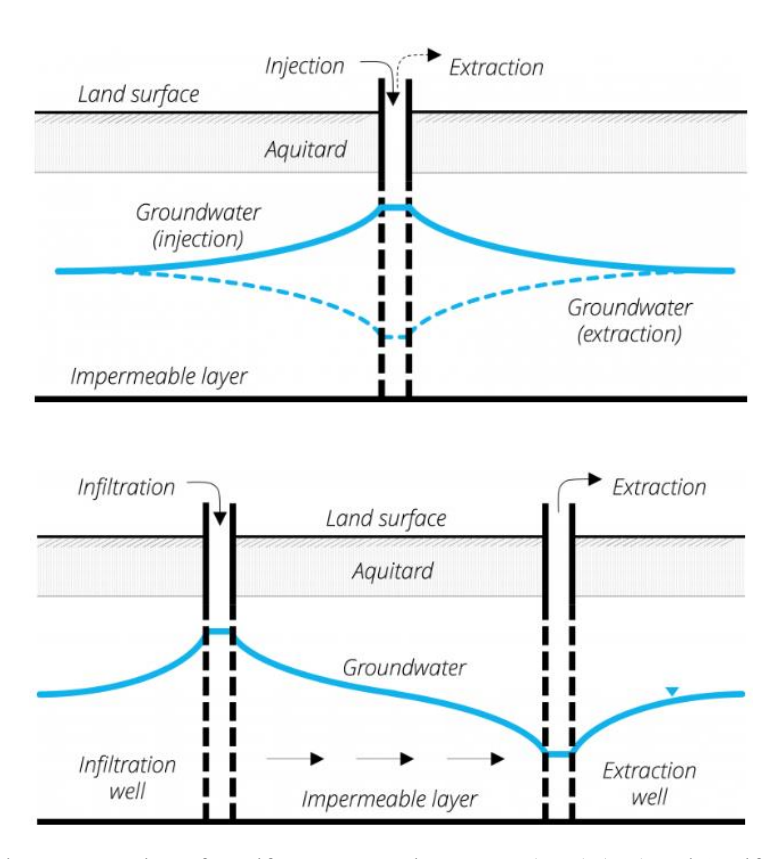


Figure 1. Schematic representation of Aquifer Storage and Recovery (ASR) (top) and Aquifer Storage, Transfer and Recovery (ASTR) (bottom) [30], [31]

#### 3.3.2 Spreading methods

Spreading methods are the most cost-effective and common MAR techniques [18]. Their main objective is to augment the gravitational infiltration and percolation of water into unconfined aquifers. In order to achieve this, structures designed to retain water are built at ground level or above [28]. These methods comprise soil aquifer treatment (SAT) and infiltration ponds. Infiltration ponds represent one of the most commonly implemented MAR methods worldwide [32]. They consist of basins that can be either excavated in the ground or constructed on open land surrounded by embankments [18]. Despite their simplicity, infiltration ponds present some disadvantages: they occupy significant land surface and often experience algal proliferation [16]. Similarly, SAT recharges aquifers through filtration under controlled conditions [33]. This method is used with treated sewage water, which passes through the unsaturated soil zone, facilitating the removal of pathogens and nutrients [16]. SAT aims to achieve both water storage and treatment.

In Figure 2, schematic representations of infiltration ponds and SAT techniques are presented.

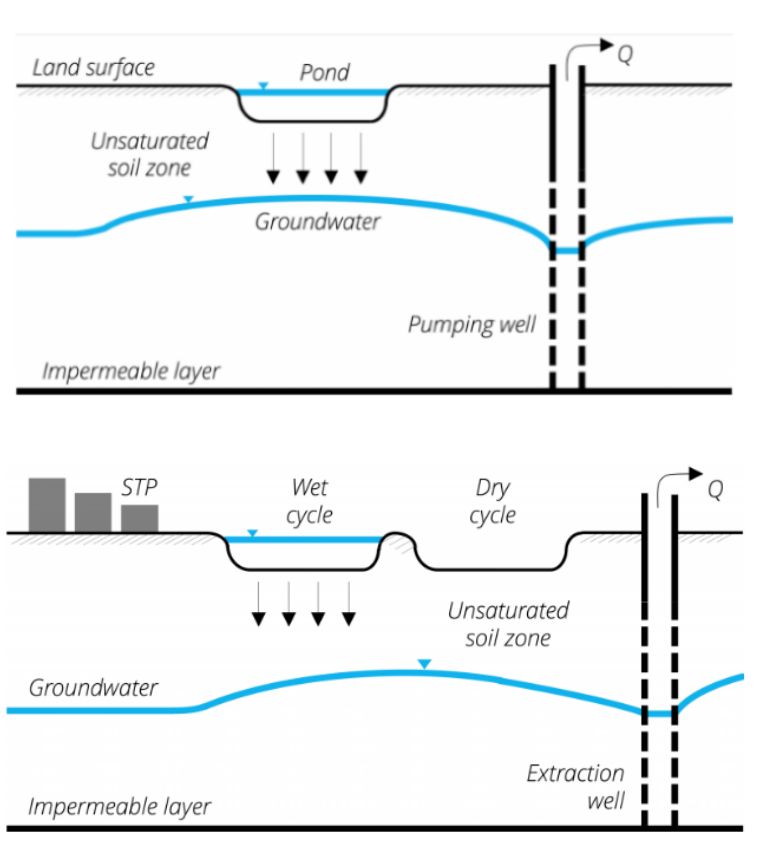


Figure 2. Schematic representation of Infiltration ponds (top) and Soil Aquifer Treatment (SAT) (bottom) [32], [33]

#### 3.3.3 Induced bank filtration

Induced bank filtration methods are used to increase the water quality of surface water in rivers or lakes [34]. They work by pumping groundwater from wells placed near these water bodies, to enhance surface water infiltration into the aquifer, thereby improving the quality of extracted water [18]. This process helps remove dissolved and suspended pollutants and pathogens by chemical, physical and biological processes, as the subsoil act as a filter [34]. A variant of this method is the induced dune filtration. In this case, the surface water to be filtered is stored in ponds constructed within dunes before infiltration [20].

In Figure 3, schematic representations of river/lake bank infiltration and dune infiltration techniques are presented.

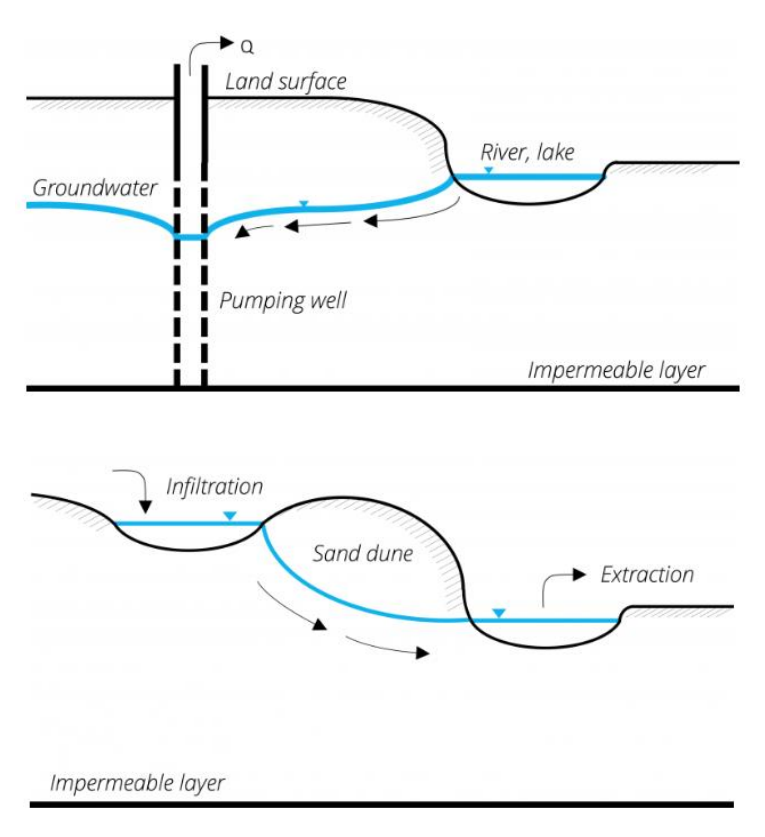


Figure 3. Schematic representation of River/lake bank infiltration (top) and Dune filtration (bottom) [34], [35]

#### 3.3.4 In-channel modifications

In-channel modifications involve constructing structures that alter streams, rivers or canals [18]. Their goal is to intercept or delay water runoff, primarily through the construction of dams [28]. In doing so, the residence time and the flow length are increased, enhancing percolation through the soil and raising the water table [17]. In-channel modifications are mainly applied within non-perennial streams and well-defined rainy season [28]. Examples include subsurface dams and

sand dams. Subsurface dams consist of barriers of low permeability located underground, designed to reduce or stop the lateral groundwater flow [36]. The barrier is made of low-permeability material [20]. Sand dams are built on low permeability lithology, and they are meant to retain both water and sediment creating an artificial aquifer upstream of the dam [20], [37]. In Figure 4, schematic representations of subsurface dams and sand dam techniques are presented.

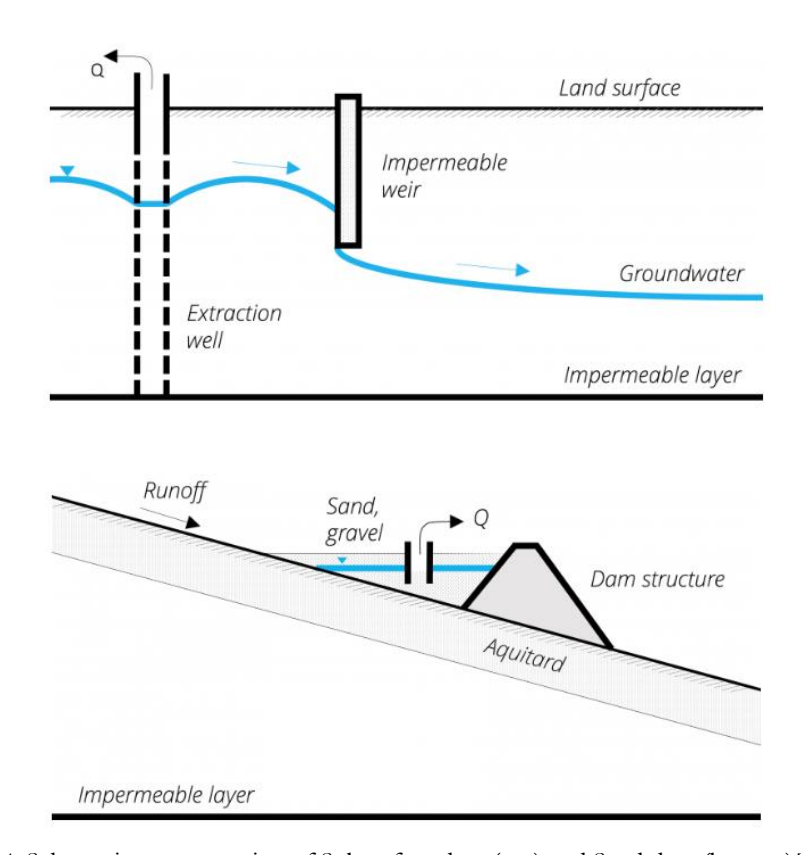


Figure 4. Schematic representation of Subsurface dam (top) and Sand dam (bottom)[36], [37]

#### 3.3.5 Rainwater and runoff harvesting

Rainwater and runoff harvesting is a simple and economical MAR method largely diffused in rural areas [17]. It involves capturing rainwater and channelling it to percolation pits to increase the infiltration of rainwater into the aquifer [18]. One of the simplest implementation is the rooftop rainwater harvesting, especially common in urban areas [38].

In Figure 5, the schematic representation of rooftop rainwater harvesting technique is presented.

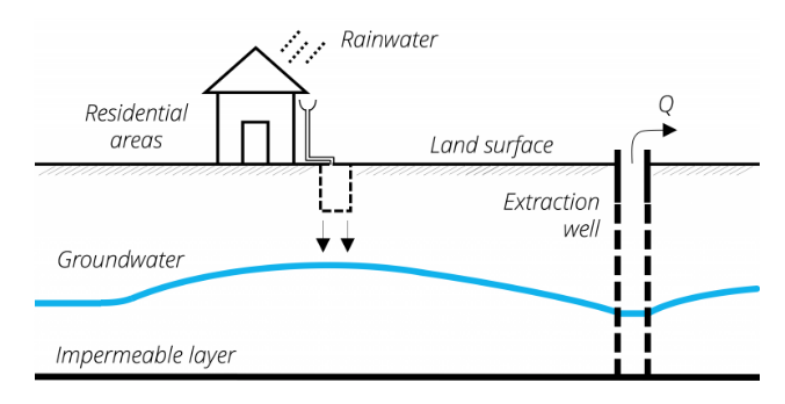


Figure 5. Schematic representation of Rooftop rainwater harvesting [38]

#### 3.4 Implementation of MAR Worldwide

To illustrate examples from the wide range of MAR applications across various fields and countries, this section presents three case studies found in the literature.

#### 3.4.1 Securing water supply to Windhoek, Namibia

The MAR systems implemented in Windhoek, Namibia, were primarily aimed at maximizing the use of the aquifer's available storage capacity to enhance water supply security.

Namibia is one of the most arid countries south of the Sahara Desert, with an average annual rainfall of just 360 mm and an annual evaporation rate of 2,170 mm. As a result, the country faces a persistent water deficit, exacerbated by the absence of perennial rivers within its borders. Moreover, the population of Windhoek is expected to reach 790,000 inhabitants by 2050, with annual water demand projected to increase from 28 Mm³/yr to approximately 50 Mm³/yr. To address this challenge, the MAR project was first studied in the 1990s. Over the previous decades, the groundwater table had dropped by 40 m, leading to a significant water supply shortage. Between 1997 and 1999, four boreholes injection tests were conducted, successfully infiltrating a total volume of 450,300 m³ of water. Following the success of the initial injection tests, additional boreholes were drilled, and within ten years the piezometric surface returned to the levels comparable to those prior to the 1950s. The project's effectiveness was demonstrated during the severe drought that struck the city from 2014 to 2015, when the high abstraction levels were sustained solely thanks to the MAR system [39].

#### 3.4.2 Soil aquifer treatment to protect coastal ecosystem in Agon-Coutainville, France

In this case, a SAT system was implemented in Normandy, France, to enhance the water quality and prevent the saltwater intrusion, thereby preserving the local coastal ecosystem.

The source water comes from a wastewater treatment plant, which can treat and infiltrate approximately 2,000 m<sup>3</sup>/day. The volume infiltrated varies throughout the year, depending on

the season and holiday periods. Recharge is performed through three infiltration ponds, which are intermittently flooded over the year. As a result, the local water table has risen by 0.5 to 1 m. The stored water is mainly used for irrigation purposes. In addition, infiltration contribute to a reduction in saltwater intrusion and an improvement in groundwater quality, meeting the site-specific water quality standards established by the government. The SAT system has turned the soil into a biogeochemical reactor, with an average residence time of about 1.8 weeks [39].

#### 3.4.3 A coastal plain groundwater reservoir in Shandong, China

Groundwater exploitation in Shandong Peninsula, China, has experienced significant growth since the 1980s, due to the rapid economic development, leading to issues such as seawater intrusion. Moreover, in the last two decades of the 20<sup>th</sup> century, the region has been hit by multiple droughts, resulting in a water shortage emergency. To address these challenges, the Water Resources Research Institute of Shandong Province and Longkou Water Authority started a MAR pilot project in 1990 in the Belisha River groundwater reservoir. The project involved the construction of a subsurface dam made by low hydraulic conductivity cement paste, designed to intercept subsurface water flows and increase storage capacity. Estimates suggest that the recharge volume ranges from 617,000 to 688,000 m³/year, while the annual extractions are approximately 600,000 m³/year, resulting in a net positive water balance. In addition to increasing the piezometric level, the project also contributed to a reduction in saltwater intrusion [39].

#### 3.5 Clogging: A Key Operational Challenge in MAR Systems

Despite the many advantages of MAR techniques, such as reduced land usage and limited evaporation losses, these systems also present some limitations. Among the most significant is clogging, which represents a major operational challenge.

Clogging in MAR systems can be categorized into four types, based on the agents responsible and on the mechanism involved: physical clogging, chemical clogging, biological clogging and mechanical clogging [18].

The main characteristics of the four types of MAR clogging are summarized in Table 2.

#### 3.5.1 Physical clogging

Physical clogging is the most common type affecting MAR structures. It is caused by the accumulation of organic and inorganic suspended solids present in the source water. There are three forms in which physical clogging can occur:

Filtration: when the particles suspended in the recharge water are larger than the pores of the permeable medium, they are filtered out and accumulate at the surface or within the pores.

- ➤ Bridging: due to collisional transport, the suspended solids collide and aggregate together into coarser particles, that can no longer pass through the pore spaces, resulting in blockage.
- Physical precipitation: when the suspended solids settle and accumulate, obstructing the pores and reducing the hydraulic conductivity.

Generally, the severity of the physical clogging is directly proportional to the concentration and size of suspended solids, and inversely proportional to the pore size of the medium [18].

#### 3.5.2 Chemical clogging

Aquifers are dynamic ecosystems where physical, chemical and biological processes interact. When the recharge water is infiltrated in the aquifer, it can alter the existing water-rock equilibrium. This disturbance can change the water quality in the aquifer, and trigger geochemical processes such as dissolution, precipitation, and other reactions, potentially reducing the aquifer permeability and leading to the chemical clogging. The occurrence of chemical clogging depends on some factors, such as the chemical composition of the recharge water and native groundwater, the mineralogy of the aquifer's rock and soil matrix, and physical conditions, like the temperature and the pressure. Chemical clogging is associated with the presence of calcium carbonate, gypsum, phosphate, iron and manganese oxide hydrates, and it usually occurs in the mixing zone of recharge water [18].

#### 3.5.3 Biological clogging

Biological clogging is the second most frequent type, after physical clogging. It is caused by the presence of algae and bacteria in the recharge water. These microorganisms, especially during infiltration, may reproduce rapidly and form a biofilm on the medium particles, reducing the hydraulic conductivity and causing the biological clogging. This phenomenon is influenced by factors including the concentration of organic carbon, nitrogen and phosphorus nutrients, temperature, pH and redox potential [18].

#### 3.5.4 Mechanical clogging

Mechanical clogging occurs when air bubbles block the pore spaces within the aquifer or screened casing of the recharge well. These bubbles may be introduced by cascading water inside the recharge well casing or by the air entering the system under negative pressure. Additionally, trapped air may stimulate the microbial growth, further worsening clogging conditions. Finally, this phenomenon can also be caused by the release of dissolved gases due to pressure or temperature changes [18].

Table 2. Summary of the main clogging encountered in MAR

Type of Clogging	Cause	Mechanism	Influencing Factors
	Suspended organic and inorganic solids	Filtration: particles are filtered out because of their size	Particle size and concentration
Physical		Bridging: aggregation of solids	Pore size of the medium
		Precipitation: settling in pores	
	Geochemical reactions altering the aquifer equilibrium		Composition of recharge water
Chemical		Precipitation of minerals	Aquifer mineralogy
			Temperature and pressure
Di-1i1	Microbial activity	Die Clas Commercia de la la Characia	Organic carbon nutrients
Biological		Biofilm formation during infiltration	pH, redox potential Temperature
N. 1 . 1	Entrapped air or gas release	Air bubbles block pore spaces or casing	Water entry conditions
Mechanical		screen	Pressure and temperature changes

#### 4 LEGISLATIVE FRAMEWORK

This chapter aims to define the legislative context surrounding MAR technologies at both international and national levels, and it is resumed in Table 3.

At a global scale, organizations such as the United Nation (UN), have established objective and guidelines for the sustainable management of water resources. Within the European Union, the main legislations regulating the MAR are Directive 2000/60/CE, regarding the safety of the water, and Directive 2006/118/CE, which specially addresses groundwater. These directives led to the development of the Italian Environmental Code (Legislative Decree No. 152/2006), and, subsequently, to the Ministerial Decree 100/2016, which rules the aquifer recharges in Italy.

#### 4.1 International Overview

In the international context, the main organizations dealing with environment issues, agree on the need to strengthen efforts towards more sustainable water management.

In 2015, all UN Members States adopted the 2030 Agenda for Sustainable Development, which sets out 17 goals aimed at improving the quality of life and equity on a global scale, both in the present and for the future generations. The main objective of the Agenda is to eradicate poverty and reducing inequalities, while at the same time promoting economic growth and social cohesion, tackling climate change, and safeguarding the environment. [40]. Among the Sustainable Development Goal (SDG), SDG 6 is of special relevance to water management, as it appeals for ensuring the availability and sustainable use of water resources for all. This goal highlights the growing pressure on the hydraulic cycle and the social and economic issues deriving from it. SDG 6 promotes the optimization of water use efficiency at all levels and across all sectors, supporting transboundary cooperation [41], [42].

At the European scale, the international commitment has led to the adoption of several Directives addressing water management. Among them, Directive 2000/60/CE, also known as Water Framework Directive (WFD), provides the basis of the European water policy. It establishes a framework for the protection of water bodies, with the dual objective of preventing further deterioration and improving the status of aquatic ecosystems. The WFD defines a series of environmental objectives for the protection of surface waters, groundwater and protected areas. With respect to groundwater, it requires Member States to adopt measures aimed at preventing pollutant dispersion in the aquifer, improving groundwater quality, and ensuring a sustainable balance between abstraction and recharge. Importantly, Part B of Annex VI, mentions artificial recharge of aquifers as one of the measures which Member States can implement in order to achieve the Directive's objectives [43].

Subsequently, the European Union adopted the Directive 2006/118/CE, commonly referred to as Groundwater Directive (GWD). This Directive is complementary to WFD, by placing the focus on the protection of groundwater resources, with the aim of preventing and limiting the introduction of pollutants in the aquifers. To achieve this goal, GWD sets criteria for the evaluation of groundwater chemical status and defines both quality standards and threshold values for several key pollutants, such as nitrates, pesticides, and certain heavy metals. According to the Directive, every MAR must not lead to the exceedance of quality standards or threshold values. Moreover, any MAR project must be supported by a monitoring programme, planned to evaluate the recharge impacts on the aquifer [44].

Taken together, the Water Framework Directive and Groundwater Directive, constitute the basis for the groundwater protection in the European Union. While WFD provides a general outline for the protection of all water bodies, GWD integrates it focusing on groundwater, establishing quality standards and threshold values. In the context of MAR, these Directives are of particular significance, as WFD recognize MAR as a valid technique to improve the aquifer water quality, and GWD guarantees that these interventions are carried under specific constraints to ensuring the long-term protection of the aquifers [43], [44].

#### 4.2 The Italian Framework

The Italian government transposed the Water Framework and Groundwater Directives through the Legislative Decree 152/2006, commonly known as Testo Unico Ambientale (TUA), and the subsequent Ministerial Decree 100/2016 (MD 100/2016). While the European Directive establishes general objectives and criteria, the TUA and the MD 100/2016 convert them in operational regulations at national level.

The TUA, enacted on 3 of April 2006, is the basis of the Italian environmental law, covering water, air, wastes and soil protection. Its Part III directly implements the WFD, with the same objectives, such as the protection of water bodies from pollution and degradation, with a long-term perspective. Within this part, Article 104 regulates water discharges into the subsoil and aquifers, by a generale prohibition but allowing specific exceptions. Among them, paragraph 4-bis grants the competent authorities the possibility to authorise discharges aimed at aquifer recharge or groundwater quality enhancement [45].

The criteria for granting such authorisations, are given by MD 100/2016, which additionally identifies MAR techniques as a supplementary measure to achieve a good groundwater status. According to this decree, MAR may be applied to aquifers deteriorated in water quality or affected by a declining piezometric levels. The source water must comply with good chemical

status and respect the environmental quality standards and thresholds established in TUA. The MAR authorisations are issued by competent authorities, such as Regions and Autonomous Provinces [46].

The value of MAR techniques under emergency scenarios is emphasised by Decree-Law 39/2023, also known as Drought Decree, and the subsequently conversion into Law 68/2023. In particular, Article 3 of the law, requires the authorities to identify the aquifers which are suitable for the MAR implementations, in order to preserve the water sources conditions [47], [48].

Table 3. Legislative Framework

Level	Legislation	Year	Main Objectives	Relevance to MAR
International	UN 2030 Agenda for Sustainable Development (SDG 6)	2015	Ensure availability and sustainable water management	Promotes sustainable water management practices and encourages actions to enhance groundwater recharge and protection
European	Water Framework Directive (WFD)	2000	Establish a framework for surface water and groundwater	Recognises MAR as a tool to reach the Directive's objectives
Union	Groundwater Directive (GWD)	2006	Protect groundwater preventing the emission of pollution	Requires monitoring and compliance with quality standards for MAR project to protect aquifers
	Testo Unico Ambientale (TUA)	2006	Transposes EU Directives regulating groundwater protection and discharges	Article 104 regulates water discharges into the subsoil authorising them for aquifer recharge or groundwater quality enhancement
Italy	MD 100/2016	2016	Defines criteria for MAR authorisations	Identifies MAR as a measure to achieve good groundwater status and specifies conditions for MAR implementation
	Drought Decree	2023	Strengthen water management under emergency conditions	Highlights the strategic role of MAR in drought mitigation and groundwater resource preservation

# 5 SeTe-ALCOTRA PROJECT

The SeTe (Sécheresse et Territoires) project is a cross-border initiative between Italy and France with the purpose of mitigating the adverse effects of extreme events such as droughts and floods, in order to protect both natural and urban environments. It was developed within the framework of the European Interegg ALCOTRA (Alpes Latines COopération TRAnsfrontalière), a transboundary programme developed by the European Union and financed by ERDF (European Regional Development Fund). The programme seeks to strengthen cooperation among European Member States, in order to address environmental, economic, and social challenges more effectively [49], [50], [51].

The SeTe project is led by the Province Administration of Imperia and involves the collaboration of six additional partners, among which the Province Administration of Cuneo. Its main objective is to promote more efficient water management practices, thereby increasing territorial resilience to extreme climatic events, while raising awareness in the local communities. Among the actions proposed, the project includes a feasibility study of MAR in the Province of Cuneo. This area has been severely affected by droughts in recent years. In 2022, Piedmont experienced the worst water scarcity in the last 75 years. The planned MAR systems are intended to enhance the aquifer storage outside of the irrigation season by exploiting the water coming from the Alps, thereby ensuring a more stable water supply throughout the year [50], [51].

This thesis focuses primarily on two aquifer recharge infrastructure located in Beinette and Tetti Pesio.

This section presents the geological, hydrological and hydrogeological framework of the region, together with the instrumentations and infrastructures adopted for the study.

### 5.1 Geological Framework

The Tetti Pesio and Beinette MAR systems are located in southern Piedmont, specifically within the Cuneo Plain. This area is composed of alluvial deposits, derived from the inputs of foothill torrents, whose dynamics was influenced by oscillations associated with different glacial periods. The Cuneo Plain is identified as a subsiding basin with a N-S axis, resulting from the uplift processes that have affected the south of the region [52].

According to ARPA, five main series of deposits can be distinguished in the area:

Fluvial Deposits Series: subdivided into recent to actual (consisting of unconsolidated sediments, predominantly gravelly-sandy and subordinately silty-clayey, of fluvial and fluvioglacial origin, often characterized by strongly cemented levels), and middle to

ancient (composed of unconsolidated sediments, gravelly-sandy and silty-clayey, also occurring in alternation).

- ➤ Glacial Deposits Series: highly heterogeneous sediments.
- ➤ Villafranchian Transition Deposits Series: mainly lacustrine, palustrine, and fluvial, outcropping at the foot of the Alpine. They form a lithostratigraphic complex characterised by the alternation of permeable and impermeable layers.
- ➤ Marine Deposits Series: primarily fine-grained sediments, such as sandy successions and clayey horizons.
- ➤ Limestones, Dolostones, and Dolomitic Limestones: these rocks are characterised by significant groundwater circulation due to the development of both shallow and deep karst processes.

The MAR sites are located in the hydrological right of the Stura di Demonte River. In this area, the superficial sequence is constituted of Fluvial Deposits, of gravelly–pebbly nature with a sandy matrix, while clay layers become more frequent at greater depths.

Finally, the lithological units are divided in three categories:

- Current alluvial complex: including the unit of present-day gravels.
- Terraced alluvial complex: including the unit of fresh gravels, subdivided into two subunits due to the presence of terraces at different elevations.
- Main alluvial complex: including the unit of conglomerates and slightly weathered gravels [53].

#### 5.1.1 Beinette geological framework

The Beinette MAR system is located north of the urban area, within an agricultural zone. The area lies to the north of the Beinette terrace, which is characterised of Villafranchian deposits, mainly consisting in clayey–gravelly sediments.

The area form part of a plain composed of a sequence of Quaternary alluvial deposits, which overlie on clayey sediments. The Triassic basement is formed by dolomitic limestones, which are high soluble in water, leading to the formation of underground karst networks. Moreover, the pressurized water present underground, tends to emerge spontaneously through the overlaying alluvial deposits [53].

The stratigraphy was defined by analysing the results from a continuous-core drilling at borehole CNP11786, in Beinette, showed in Figure 6 [54].

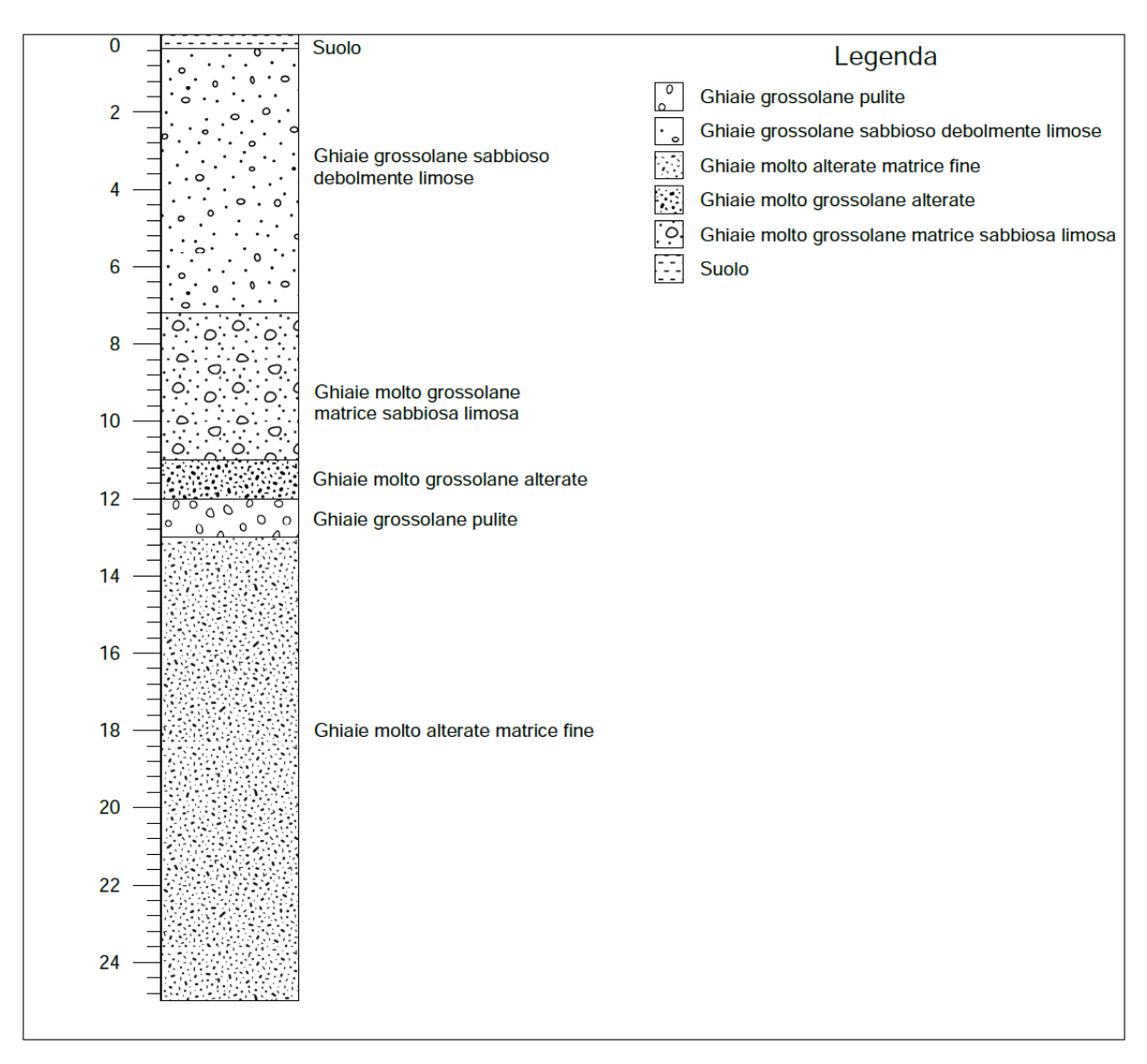


Figure 6. Stratigraphy from CC drilling in Beinette [54]

#### 5.1.2 Tetti Pesio geological framework

The Tetti Pesio MAR system area is bounded to the south by the scarp of Villafranchian deposits belonging to the Beinette plateau. To the north, clayey-gravelly sediments occur, together with the incision of the Pesio Stream, which exposes the substrate formed by the Lugagnano Clays and Miocene marls. To the west, the scarp of the Stura Stream reaches the Villafranchian deposits, which act as a permeability boundary with the overlying alluvial sediments. Along these scarps, at the transition between the Quaternary gravels and the Pliocene substrate (Villafranchian Gravels and Lugagnano Clays), numerous springs are found [53].

The stratigraphy was defined by analysing the results from a continuous-core drilling at borehole 499, in Tetti Pesio. Figure 6 shows the obtained stratigraphy [54].

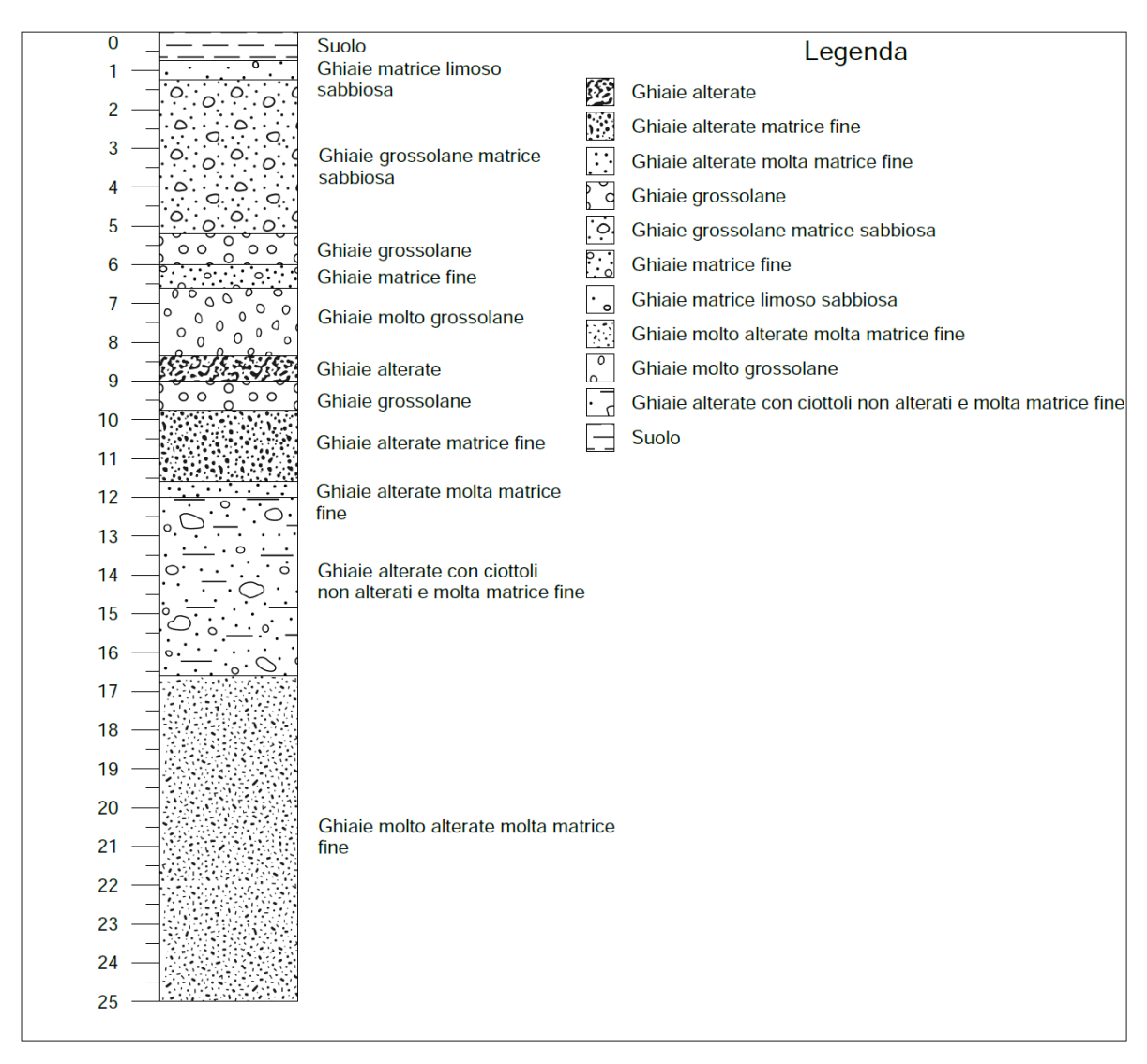


Figure 7. Stratigraphy from CC drilling in Tetti Pesio [54]

#### 5.2 Hydrogeological Framework

A common feature of the sedimentary basin in the Piedmont plains is a multi-layered aquifer system, where hydrological communication between neighbouring basins occurs mainly at the water table level, located within the mainly gravelly layers of the Upper Quaternary.

In the Cuneo plain, unconfined aquifers represent the main groundwater resource for both drinking water supply and irrigation. Among the main hydrogeological complexes, the Ancient Gravel Alluvial Complex, which includes the Beinette terrace, is composed of gravels with abundant silty matrix and well-developed silty—clayey soils. Within this unit, a shallow unconfined aquifer of limited thickness may occur.

The Main Alluvial Complex, instead, consists of fluvial and glaciofluvial deposits as well as more recent alluvial sediments. It is characterised by gravels with silty matrix alternating with sandy horizons, with thicknesses ranging from 80–90 m in the piedmont sector to only a few metres in

the distal areas. This complex hosts several unconfined aquifers, which are particularly relevant for agricultural purposes due to the presence of springs and draining trenches, including those of Tetti Pesio and the Beinette Lake area.

The Shallow Aquifer is hosted within the Pleistocene–Holocene Fluvial Deposits Series, showing higher productivity in the southern sector of the Cuneo plain, where coarser grain sizes are found. Along the main rivers, a draining effect on the water table can be observed. In the Tetti Pesio area, the phreatic contours display a marked reduction of the hydraulic gradient, coinciding with the historical alignment of springs extending towards the Beinette Lake [53].

#### 5.2.1 Beinette hydrogeological framework

The Beinette site belongs to the Main Alluvial Complex, where unconfined aquifers are recharged both by precipitation and, primarily, by substantial seepages losses from the rivers draining the Alpine valleys. In particular, the Grana, Maira, and Varaita streams experience considerable seepage losses once they reach the plain.

Approximately 2 km south of Beinette lies the Beinette Lake, the largest spring in Piedmont and the second largest in Italy. The lake is located in a slight depression and is fed by numerous underground sources, which provide a flow ranging from 1200 to 2600 l/s. Thanks to the network of channels originating from the lake, it supplies water for irrigation, fish farming, and hydroelectric power production.

The hydrographic network of the area is mainly represented by two streams:

- ➤ Colla Stream: after draining the waters from the Boves area, it flows north of Beinette and then crosses the study area from southwest to northeast, before joining the Brobbio Stream.
- ➤ Brobbio Stream: it originates from the confluence of the Brobbietto channel, which comes from Beinette Lake, and the Josina Stream. After crossing the town of Beinette and flowing south of the study area, it joins the Pesio Stream. Although with a minor effect, it drains the unconfined aquifer downstream of Beinette.

Just downstream of Beinette, several draining trenches (fontanili) are present, designed to intercept large volumes of water from the unconfined aquifer. The most important is the Fontanile dei Paschi, located between the Brobbio and Colla Streams, about 2 km east of Beinette. It consists of three branches that merge into a single channel, which eventually flows into a fish farm. The trench reaches a depth of about 6 m at its head, gradually decreasing until it meets the ground level near the fish farm. Its total discharge ranges between 800 and 1200 l/s [53].

The hydrogeologic framework of the zone is illustrated in Figure 8.

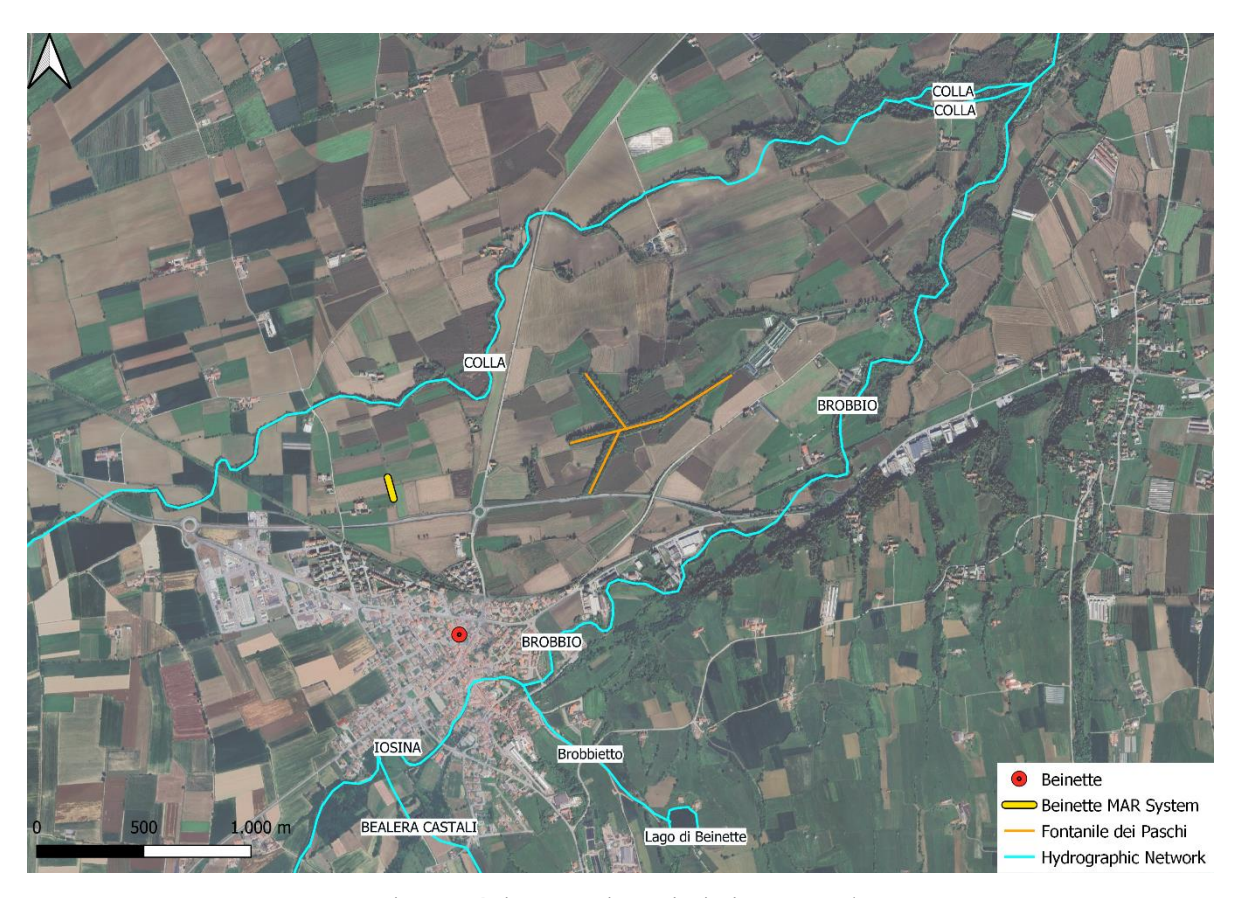


Figure 8. Beinette Hydrogeological Framework

#### 5.2.2 Tetti Pesio hydrogeological framework

Like the Beinette site, the Tetti Pesio area belongs to the Main Alluvial Complex. In this zone, several draining trenches are present, including Fontanile Comunia, Fontanile Lagot, Fontanile Tina, and Mattunotta [53].

The hydrographic network is mainly represented by the Gesso Stream, which, according to water chemistry analyses, contributes to the recharge of the unconfined aquifer on the right side of the Stura River. In addition to the contribution from the Gesso Stream, the unconfined aquifer is also recharged by irrigation practices and precipitation [54].

The hydrogeologic framework of the zone is illustrated in Figure 9.

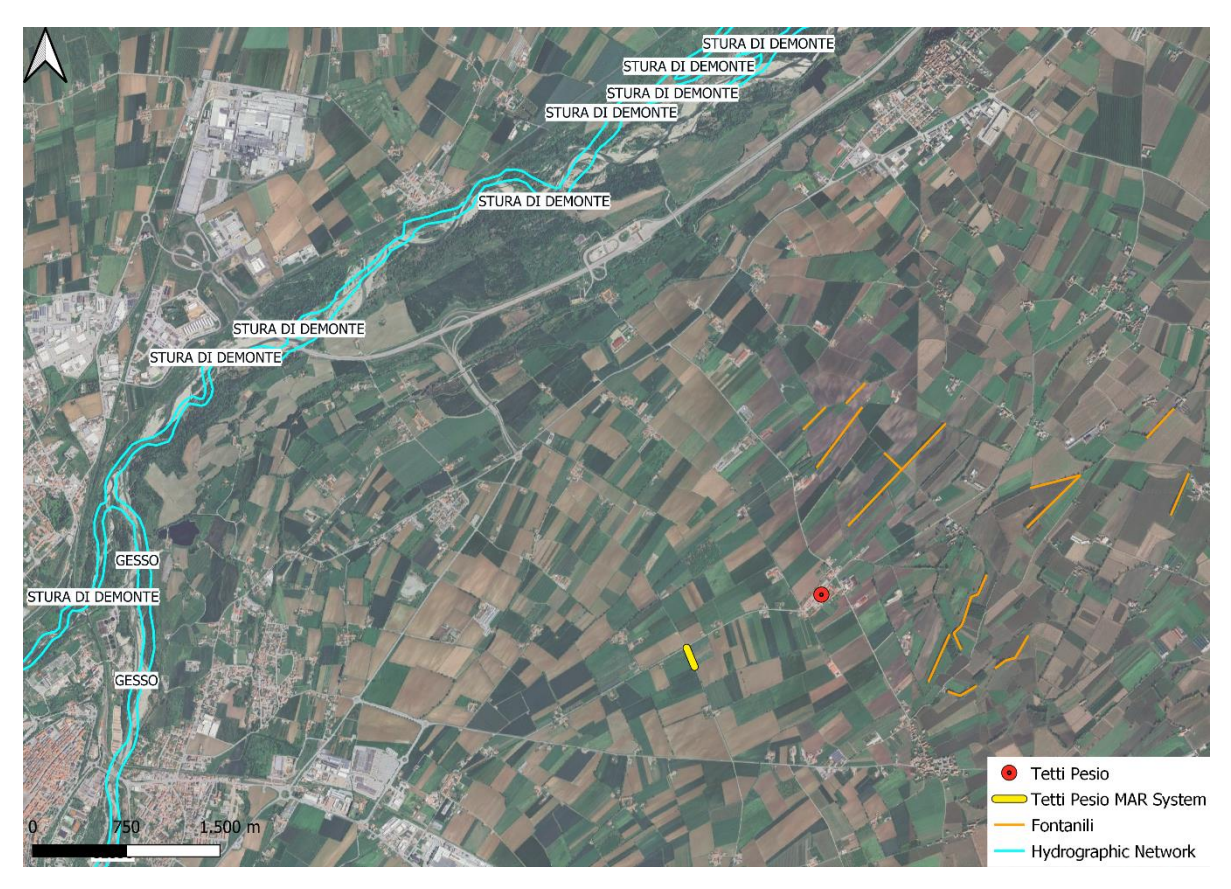


Figure 9. Tetti Pesio Hydrogeological Framework

#### 5.3 Design and Functioning of the MAR Structures

#### 5.3.1 Beinette recharge trench

Beinette MAR system is located north to the urban area of the municipality, approximately 1 km upstream from the Fontanile dei Paschi (see Figure 8). It consists of a modified irrigation channel designed to feed the aquifer. At the base of the channel, a concrete section was constructed and divided into two parts by a fine-mesh grid, preventing vegetation and debris from entering and clogging the infiltration trench.

In the lower section, one wall is equipped with a sluice gate that regulates whether the water is diverted into the trench. From the gate, a slightly upward-sloping concrete pipe conveys the flow to a concrete collection chamber, built to collect the diverted water. From the bottom of this chamber, the infiltration trench originates, running parallel to the irrigation channel for approximately 100 m, and it is perpendicular to the aquifer flow direction. The trench consists of a PVC tube surrounded by gravel and lined with geotextile, which act as filtering layers. Inside the collection chamber, a pressure datalogger was installed to continuously monitor the water level and to verify possible clogging of the structure. In addition, two broad-crested weirs were built upstream and downstream of the intake, each equipped with a pressure datalogger, allowing the discharge of the channel before and after the intake to be measured, and consequently, the

infiltrated flow to be calculated. Finally, small retaining walls were built along the channel banks immediately upstream and downstream of the weirs. Since these banks lacked vegetation cover, they were particularly prone to erosion.

To better illustrate the structure, Figure 10 provides photographs of the main elements of the intake and monitoring system.



Figure 10. Photographs taken during construction works: A) pipe connection between the collection chamber and the concrete section of the channel; B) concrete section with the fine-mesh grid installed; C) one of the two broadcrested weirs; D) sluice gate that regulates the flow to the collection chamber.

### 5.3.2 Tetti Pesio recharge trench

The Tetti Pesio MAR facility is located west to the inhabited area (see Figure 9). It also originates from the modification of an irrigation channel. In this case, the water flows directly from the channel into the recharge chamber through a lateral sluice gate, preceded by two grids that act as filters for vegetation and debris. The first grid tends to clog easily due to the presence of algae in the canal; however, its position and design allow for simple cleaning. From the bottom of the recharge chamber, the infiltration trench starts. It consists of a PVC pipe surrounded by gravel

and geotextile, oriented perpendicularly both to the groundwater flow direction and to the irrigation channel. At the bottom of the chamber, a pressure datalogger was installed to monitor the water level and to verify that the trench is not clogged. To force water from the irrigation channel into the recharge chamber, guides were installed inside the channel to allow the insertion of a sluice gate positioned perpendicular to the flow.

To provide a clearer understanding of the system, Figure 11 illustrates the key construction features.

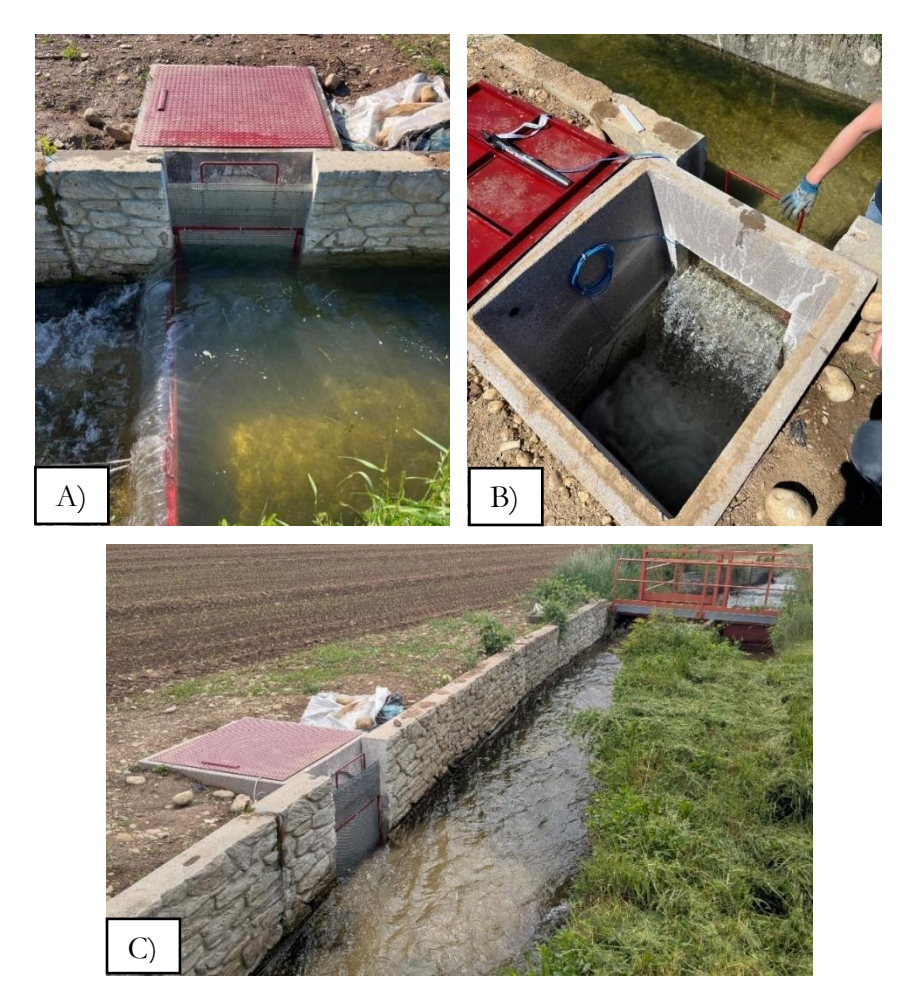


Figure 11. Photographs taken at Tetti Pesio MAR system: A) sluice gate connecting the channel to the collection chamber; B) collection chamber; C) irrigation channel integrated with the MAR structure.

# 5.4 Monitoring System of the Project

In order to evaluate the impact of the MAR projects on the underlying aquifer, in addition to the ARPA piezometers, a set of pressure dataloggers was installed in boreholes and within the channels, with the purpose of quantifying the piezometric levels and the channels flow rates. In

addition, two barologgers, one for each site, were installed to record atmospheric pressure, which was subsequently used to correct the pressure dataloggers measurements.

The use of these instruments is detailed in Chapter 6 (Methodology), while the geographic distribution of the instruments is illustrated in Figure 12-Figure 14.

Table 4 presents the pressure dataloggers used in the project, with their coordinates and elevation above sea level, while

Table 5 presents the pressure barologgers positions.

Table 4. Pressure dataloggers coordinates and elevations

Site	Datalogger Code	E coordinates (UTM WGS84 32 N)	N coordinates (UTM WGS84 32 N)	h (m a.s.l.)
-	POZZO_GRA	391500.732	4914083.95	492.084
	B01_CC	391951.506	4913675.11	488.808
DEINIETE	B02_DDN	392238.226	4914142.33	485.853
BEINETTE	B03_DDN	392612.461	4914284.22	480.858
	POZZO_SERR	391500.732	4914083.95	492.084
	Т03	392147.827	4913379.24	488.577
	POZZO_499	392060.841	4916638.78	476.65
	CAMPO_DDN	389884.66	4917350.06	488.072
TETTI PESIO	CC_TRUCCHI	392068.077	4916629.47	476.95
TEGIC	DDN_CASE	390997.216	4918125	475.972
	T02	397447	4920151	427.12

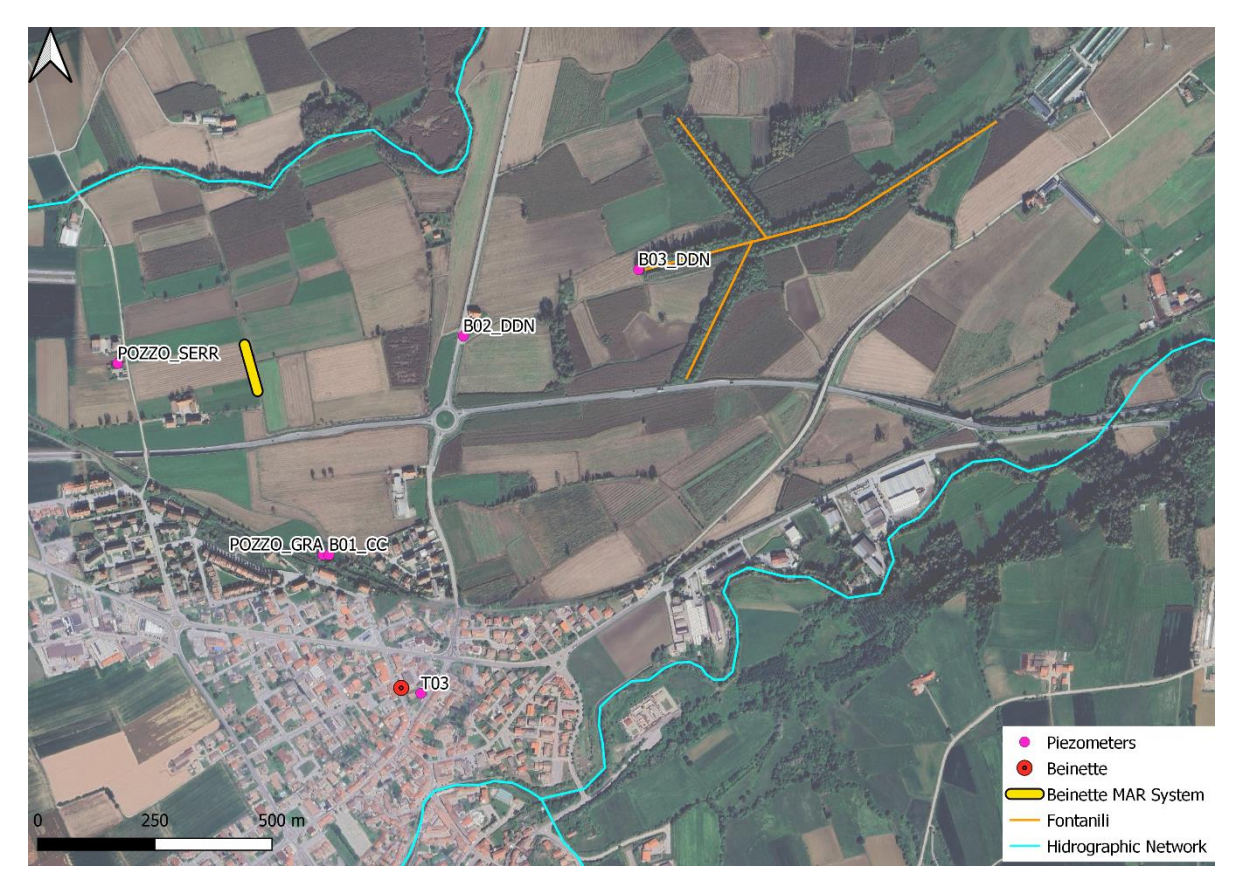


Figure 12. Dataloggers positioning in Beinette

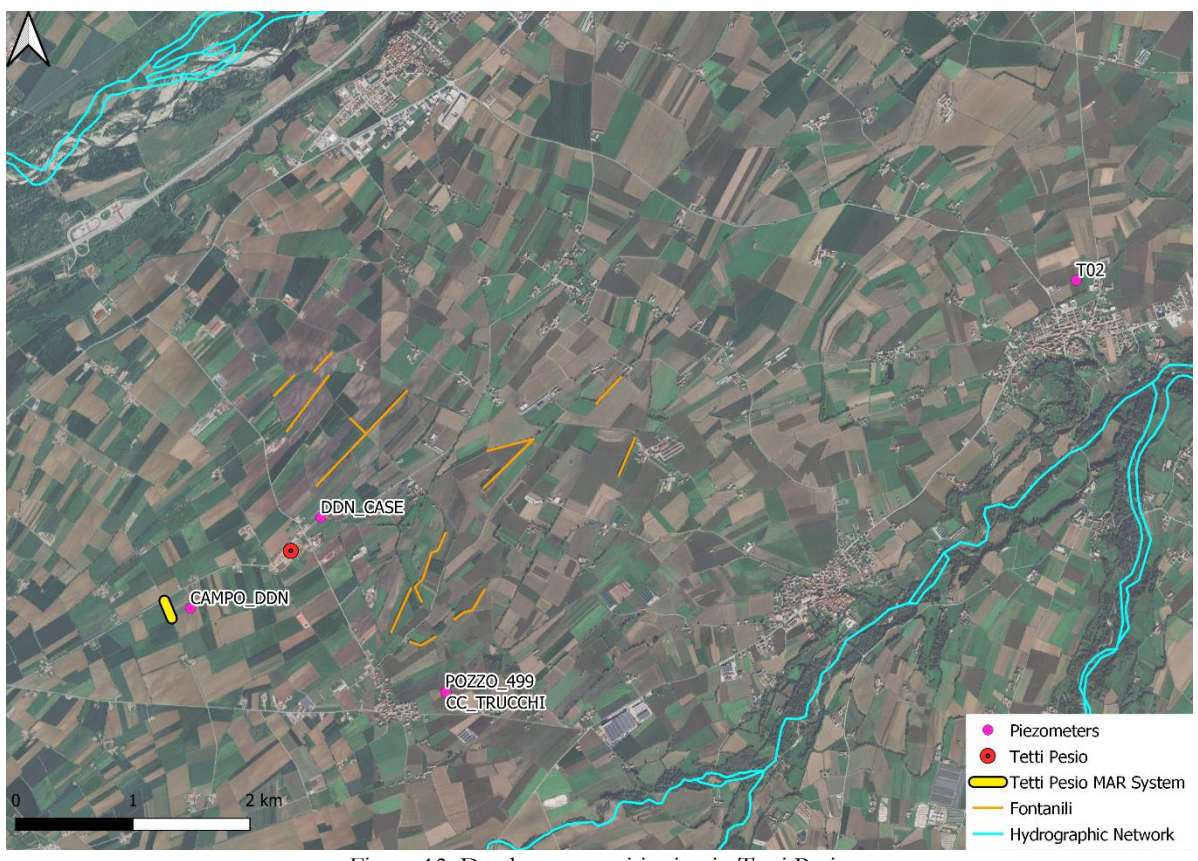


Figure 13. Dataloggers positioning in Tetti Pesio

Table 5. Barologgers coordinates

Site	Datalogger Code	E coordinates (UTM WGS84 32 N)	N coordinates (UTM WGS84 32 N)
BEINETTE	BARO_BEINETTE	392060.8409	4916638.784
TETTI PESIO	BARO_TETTIPESIO	391951.506	4913675.109

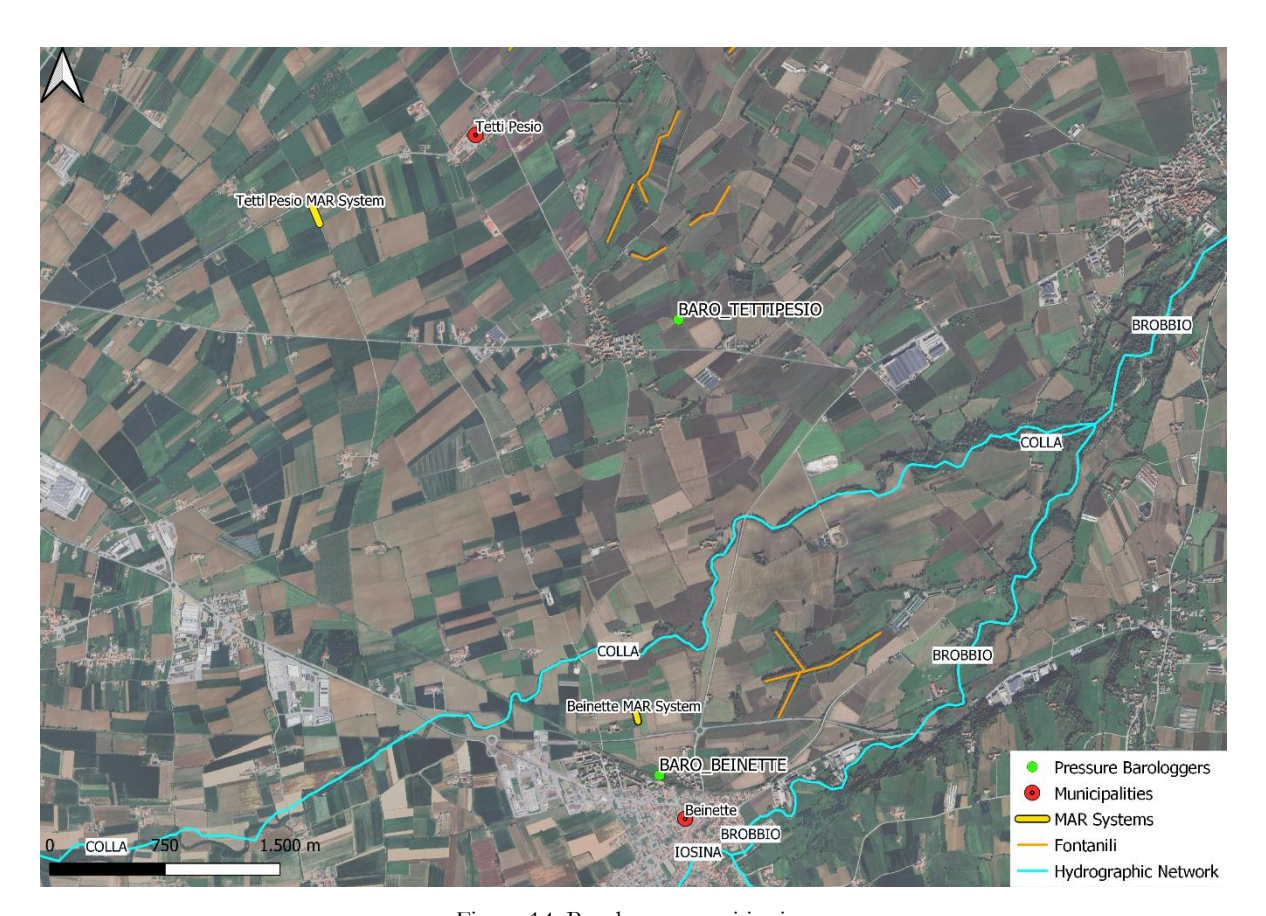


Figure 14. Barologgers positioning

## 6 METHODOLOGY

In this section it is presented the methodology followed during the study of the Beinette and Tetti Pesio MAR infrastructures.

## 6.1 Assessment of Infiltrated Volume

### 6.1.1 Beinette recharge trench

To evaluate the volume of water infiltrated through the Beinette recharge trench, two broadcrested weirs were constructed immediately upstream and downstream of the intake structure.

A broad-crested weir is a hydraulic structure that permits the discharged to be derived by measuring the head over the crest, taking advantage of its hydraulic properties. For a weir to be classified "broad", the crest must be sufficiently long for the streamlines to become parallel to the crest. Under these conditions, the pressure distribution above the crest is hydrostatic, and the critical flow depth occurs on the weir crest.

To establish the relationship between the head of the crest h and the discharge Q, the software WinFlume 2.1, developed by the U.S. Department of Agriculture, was employed. Using this relation, it was possible to calculate the volume of the infiltrated water.

### 6.1.1.1 Determination of water levels

The head over the crest was continuously monitored using two pressure dataloggers, one for each weir. The instruments were installed inside PVC pipes anchored to the channel wall, immediately upstream of the weirs. It was assumed that the water level at this location corresponded to that on the crest. Direct installation on the crest was not feasible because, under certain discharge conditions, the head was only few centimetres, making it impossible for the instruments to detect. The PVC pipes served to create a stilling zone, thereby enabling more reliable measurements of the water level.

The pressure measured by the dataloggers is the sum of the atmosphere and hydrostatic pressure. Therefore, the first step consisted in the removal of the atmosphere pressure, which was continuously recorded by barometer BARO\_BEINETTE, installed near the Beinette trench (see Figure 14). Given the proximity, it was assumed to be representative of the site conditions. The measured atmosphere pressure is plotted in Figure 15.

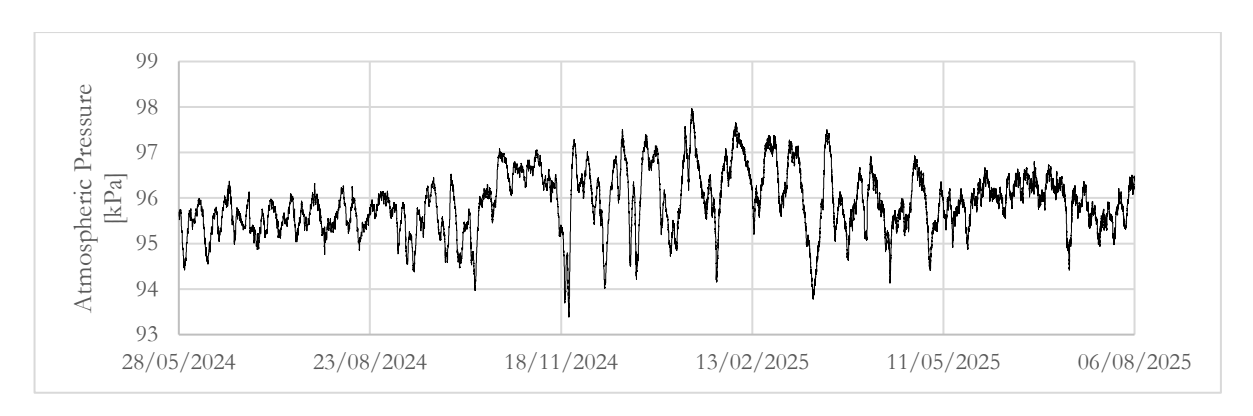


Figure 15. Atmospheric pressure in kPa measure by BARO\_BEINETTE

Pressures were converted in equivalent meters of water, in order to simplify the calculation. Through the Stevin law (1), it was possible to calculate the pressure of 1 m of water column.

$$p = \rho g h \tag{1}$$

with

- p = pressure at the considered point [kPa]
- $\rho$  = water density [kg m<sup>-3</sup>]  $\sim 1000$
- $g = \text{gravity acceleration [m s}^{-2}] \sim 9.806$
- h = fluid column over the considered point [m]

It resulted that 1 m of water column corresponds to  $9.806 \, kPa \, m^{-1}$ . Hence, all data from dataloggers and barometers were divided per  $9.806 \, kPa \, m^{-1}$  to obtain equivalent water depth. Since the dataloggers could not be installed directly on the crest of the weir, a calibration procedure was performed. The offset between the datalogger sensor elevation and the crest elevation was determined by comparing the datalogger readings (hC) with manual measurements of water head above the crest (h), taken simultaneously. This offset was subtracted from the water level recorded by the datalogger to obtain the actual head over the crest.

The scheme of the offset calculation is shown in Figure 16.

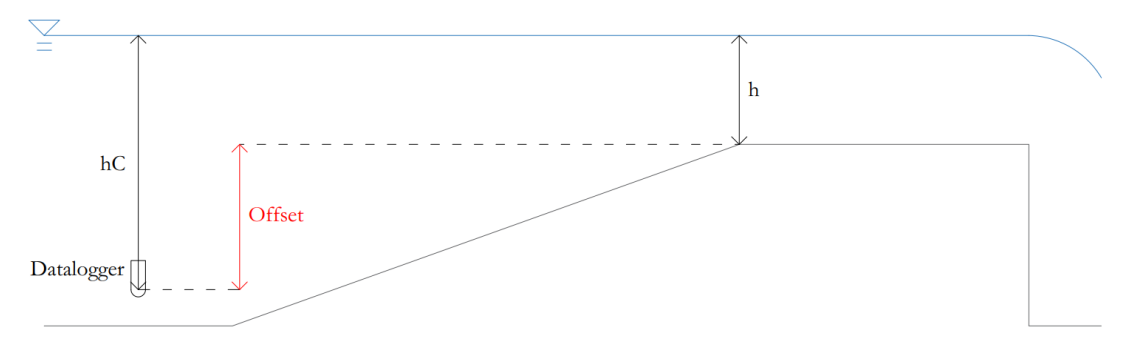


Figure 16. Schematic view of the datalogger offset

## 6.1.1.2 Determination of the **h-Q** equation

In order to obtain the flowrate of the channel from the head over the crest of the weirs, the software WinFlume 2.1 was employed.

The first step was the reconstruction of the geometry of the channel and of the weirs, shown in Figure 17-Figure 19.

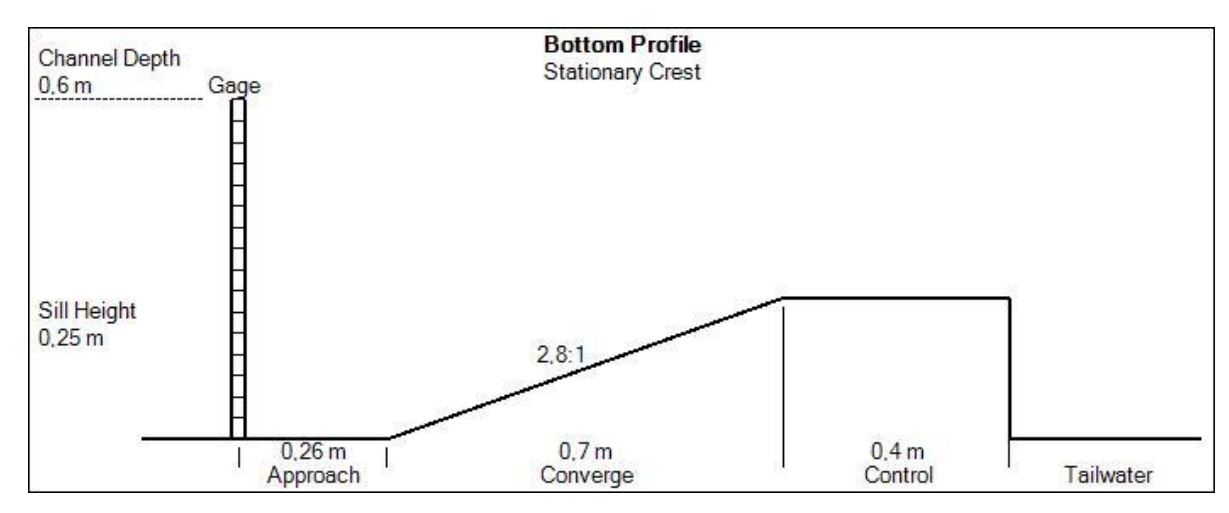


Figure 17. Longitudinal profile of the upstream broad-crested weir in the Beinette MAR system

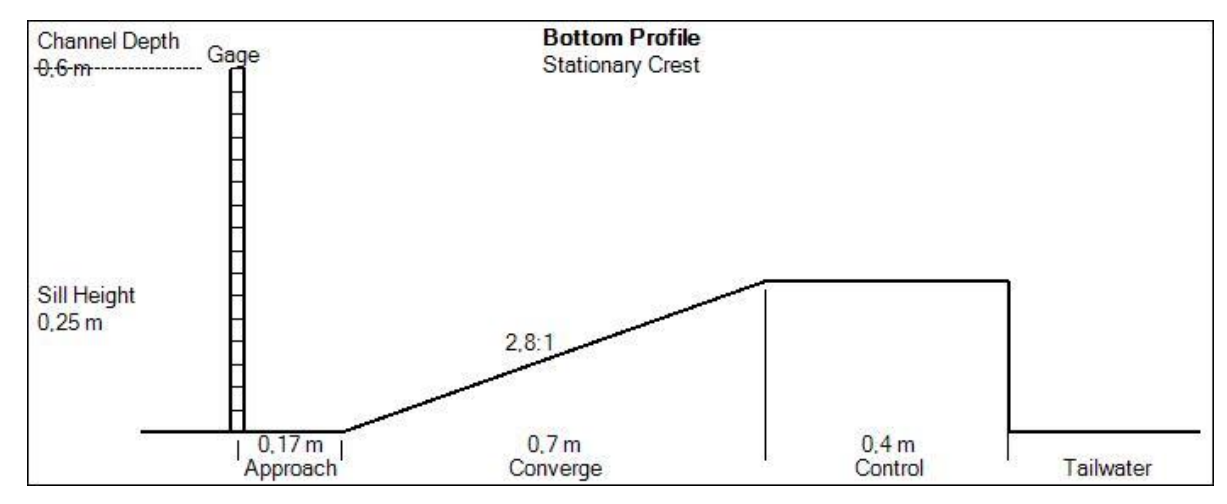


Figure 18. Longitudinal profile of the downstream broad-crested weir in the Beinette MAR system

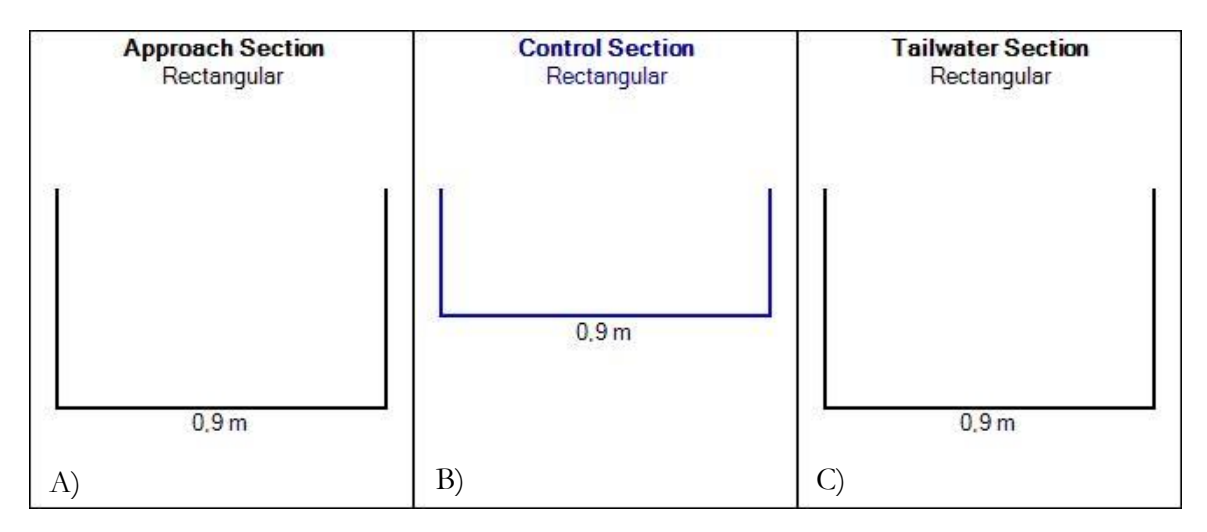


Figure 19. Cross-sections of the upstream and downstream weirs: (A) Approach section; (B) Control section; (C) Tailwater section

Subsequently, some hydraulic parameters, including the definition of the slope S, the Manning number n and the roughness height  $\epsilon$ , were defined. S was derived thanks to GPS acquisition and resulted equal to  $0.003~mm^{-1}$ , while n was assumed to be 0.033 and  $\epsilon$  equal to 0.0015~m, consistent with the rough concrete material of the weir.

Winflume computes the h-Q relation assuming that:

> The critical depth occurs on the weir crest.

$$h = y_c \tag{2}$$

 $\triangleright$  The Froude number Fr is equal to 1

$$Fr = \frac{V_c}{\sqrt{gy_c}} = 1 \tag{3}$$

The energy between the upstream section,  $H_1$ , and the crest of the weir,  $H_2$ , is conserved, i.e. head losses are neglected.

$$H_1 = H_2 \tag{4}$$

The specific energy is expressed as:

$$H_a = h_a \frac{V_a^2}{2g} \tag{5}$$

Through iterative hydraulic computations, Winflume derives an empirical equation that relates h and Q, of the form:

$$Q = k * h^u \tag{6}$$

where k and u are coefficient derived from the calibration of the weir geometry.

### 6.1.1.3 Assessment of the infiltrated volume

Once the *h-Q* correlation for both weirs were established, the discharge was calculated at 15-minutes intervals, corresponding to the datalogger acquisition frequency.

The infiltration discharge  $Q_{in}$  was determined subtracting to the upstream flowrate  $Q_1$  the downstream flowrate  $Q_2$ .

$$Q_{in} = Q_1 - Q_2 \tag{7}$$

The infiltrated volume was then obtained by the time integration of the infiltrated discharge. Assuming that  $Q_{in}$  remained constant within each acquisition interval,  $\Delta t = 15$  min, the volume infiltrated between two consecutive measurements is given by

$$V_{in} = Q_{in} * \Delta t \tag{8}$$

The cumulative infiltrated volume was obtained as the sum of all intervals over the study period.

$$V_{tot} = \sum V_{in} \tag{9}$$

### 6.1.2 Tetti Pesio recharge trench

To evaluate the volume of water infiltrated through the Tetti Pesio MAR system, the transverse sluice gate installed at the intake was used as a hydraulic control structure. The method relies on comparing the discharge upstream of the intake with the discharge overflowing the sluice gate, with their difference corresponding to the infiltrated flow.

To establish the relationship between water levels and discharge, rating curves were developed through field measurements with a current meter. Using these curves, the continuous records of pressure dataloggers allowed the estimation of upstream and downstream discharges, and thus of the infiltrated volume.

### 6.1.2.1 Determination of water levels

The water levels in the channel and at the sluice gate were measured through two pressure dataloggers: one installed approximately 30 m upstream of the intake, far enough not to be affected by the structure, and one positioned close to the transverse sluice gate (Figure 20). In the latter case, it was assumed that the recorded water level corresponded to the level at the sluice gate position, an assumption verified through field measurements.



Figure 20. Plan view of the channel showing datalogger arrangement

As already described in Section 6.1.1.1, the atmospheric pressure was subtracted, from the dataloggers records, in order to obtain the actual water head. Atmospheric pressure was measured by the barometer BARO\_TETTIPESIO, located near the trench (Figure 14), and therefore considered representative of the site conditions.

Figure 21 reports the atmospheric pressure recorded by BARO\_TETTIPESIO.



Figure 21. Atmospheric pressure in kPa measure by BARO\_TETTIPESIO

To use the sluice gate as a weir, it was necessary to determine the head over the crest h. This was obtained by subtracting the sluice gate height  $h_{sluice}$  (0.31 m) from the water level measured by the datalogger hC, already corrected with the offset, since it was not possible to install it directly on the bed of the channel, as previously explained in Section 6.1.1.1.

$$h = hC - h_{sluice} \tag{10}$$

A schematic representation of the datalogger installation at the sluice gate is provided in Figure 22.

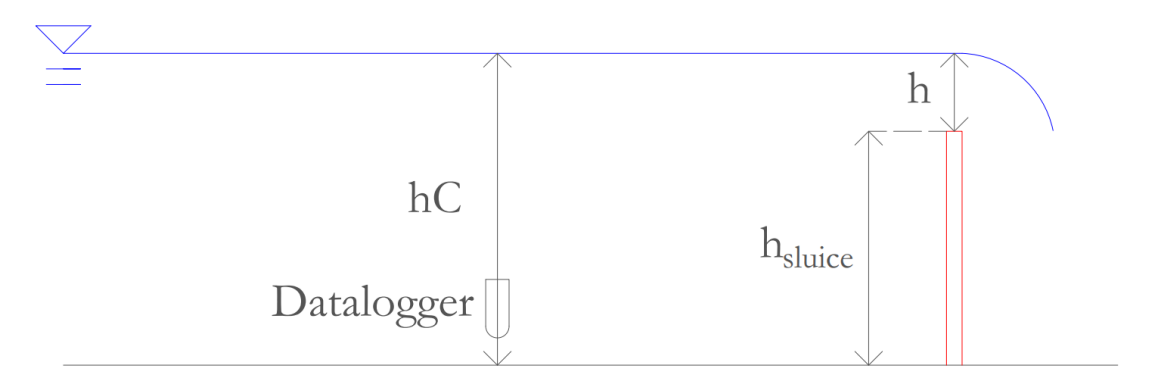


Figure 22. Schematic view of the measurements for the calculation of the head over the crest

### 6.1.2.2 Development of rating curves

To convert the water level measurements recorded by the dataloggers into discharge values, two rating curves were developed, one for each monitoring point. This was achieved by correlating four discharge measurements in the channel with the corresponding four water levels recorded by the upstream datalogger, as well as with the four simultaneous measurements of the head over the sluice gate.

The discharge measurements were obtained using a current meter. For each measurement campaign, the channel cross-section was ideally divided into a grid (Figure 23), and in the centre of each subdivision s, three velocity readings were taken. The mean velocity  $v_{mean,s}$  of the three readings was assigned as the representative velocity of the subdivision. This velocity was then multiplied by the corresponding area  $A_s$ , providing the partial discharge  $Q_s$ .

$$Q_s = v_{mean,s} * A_s \tag{11}$$

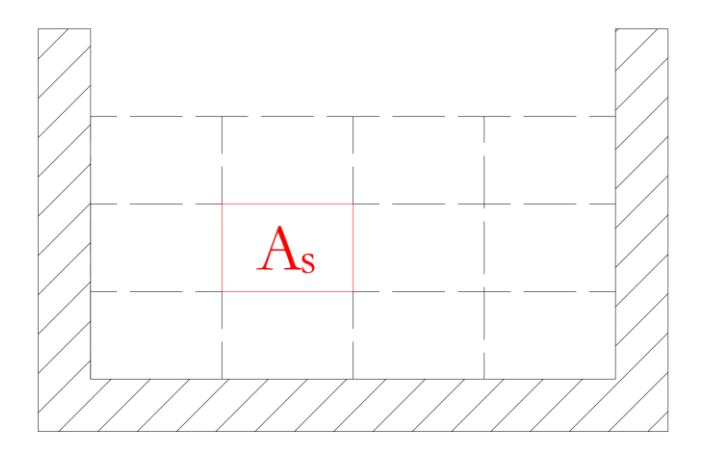


Figure 23. Example of the ideal grid for the flowrate measurements

The total channel discharge  $Q_{tot}$  was obtained as the sum of all partial discharges.

$$Q_{tot} = \sum Q_s \tag{12}$$

The total discharge values were subsequently correlated with the simultaneous water level measurements at the upstream datalogger and with the head over the sluice gate. A power regression was applied to derive the rating curves (h - Q) for both points, together with their corresponding equations, in the form of:

$$O = a * h^b \tag{13}$$

### 6.1.2.3 Assessment of the infiltrated volume

Using the h-Q relations derived previously, the 15-minute records from the dataloggers allowed for a quasi-continuous estimation of the upstream and downstream discharges,  $Q_1$  and  $Q_2$ . The infiltrated flowrate  $Q_{in}$  was derived as the difference between the upstream and downstream discharges.

$$Q_{in} = Q_1 - Q_2 \tag{14}$$

It was assumed that the water level measured by the dataloggers remained constant within each interval  $\Delta t = 15 \, min$ ; therefore, by multiplying the discharge by the time step, the corresponding volume  $V_{in}$  was obtained.

$$V_{in} = Q_{in} * \Delta t \tag{15}$$

Since no automatic system was available to detect the insertion of the transverse sluice gate, and thus the actual activation of the infiltration system, the volume difference was calculated only when the downstream datalogger recorded a water level higher than the sluice gate height (0.31 m). This ensured that only periods of actual MAR operation were considered.

The cumulative infiltrated volume was finally obtained as the sum of all intervals over the study period.

$$V_{tot} = \sum V_{in} \tag{16}$$

# 6.2 Assessment of the Precipitation Contributing to Aquifer Recharges

To evaluate the actual influence of the Beinette and Tetti Pesio MAR systems on the underlaying aquifer, it was necessary to delineate the precipitation contribution areas, in order to isolate the effects of the artificial recharge.

The individuation of the basins contributing to the aquifer recharge was performed using the software QGIS 3.16, in particular with the tools r.watershed and r.water.outlet. Precipitation over the basins was then estimated through the Thiessen polygons method, based on the pluviometric stations in the area.

### 6.2.1 Basin delineation with QGIS

The analysis was carried out starting from the Piedmont DEM (Digital Elevation Model), with a spatial resolution of 50m. A DEM is a digital representation of terrain in which each pair of spatial coordinates (X, Y), is associated with an elevation value (Z).

After importing the DEM into QGIS, the r.watershed tool was applied. Developed by US Army Construction Engineering Research Laboratory, this tool can be used for calculating several useful parameters; among them, two were used for basin identification:

- > Stram segments: a vector file of water courses.
- Drainage directions: calculated based on the orientation of the gradient vector.

The drainage directions were calculated with the Single Flow Direction (SFD) approach, which assumes that subsurface flow occurs only toward the steepest downslope neighbour.

The r.water.outlet tool was subsequently employed to automatically delineate the basins, requiring only the outlet coordinates as input. For the Beinette trench, the outlet was located along the Brobbio Stream, shortly before its confluence with the Colla Stream, whereas for the Tetti Pesio trench it was placed along the Gesso River, just upstream of its confluence with the Stura di Demonte River

Table 6 reports the coordinates of the basin outlets used for the delineation.

Table 6. Basin outlets coordinates

Site	E coordinates (UTM WGS84 32 N)	N coordinates (UTM WGS84 32 N)
BEINETTE	394724	4915856
TETTI PESIO	385064	4916258

### 6.2.2 Thiessen Polygons for the basin rainfall precipitation

To quantify the basin rainfall, the Thiessen polygon method was adopted. This approach is widely used in hydrology, due to its simplicity and accuracy. As a matter of fact, it only requires the rainfall data from pluviometric stations and a weighting factor derived from the proportion of area they represent, obtained through the construction of Thiessen polygons [55].

Thiessen polygons are generated starting from the station locations, considered as generator points. Each position in space is assigned to the nearest generator point, resulting in polygons that are exhaustive, covering all the domain, and mutually exclusive, sharing only the borders. These boundaries correspond to segments of the perpendicular bisector between pairs of generators points, while vertices are given by their intersection. The underlying assumption is that all points within a Thiessen polygon share the same rainfall characteristics as the pluviometric station located inside it, specifically the precipitation height [56].

Thiessen polygons were constructed using the QGIS Voronoi Polygons tool. The total basin rainfall was then estimated as the weighted average of the precipitation measured at the stations, with the weights corresponding polygon areas.

The pluviometric stations positions and their rainfall data were obtained from the ARPA Piedmont portal and listed in Table 7.

Table 7. Pluviometric stations used for the construction of Thiessen polygons

Station Name	Code	E Coordinates (UTM WGS84 32 N)	N Coordinates (UTM WGS84 32 N)
Chiusa Pesio	1	392988.34	4898661.83
Robilante Vermenagna	2	381732.59	4902247.34
Mondovì	3	405273.4	4916496.28
Roccaforte Mondovì	4	399840.46	4907071.62
Pradeboni	5	391400.41	4905940.83
Boves	6	385355.22	4910087.21
Cuneo-Cascina Vecchia	7	382657.14	4914024.01
Cuneo-Camera Commercio	8	384624.65	4916068.71
Morozzo	9	395888	4919108
Andonno Gesso	10	375075.41	4905367.68
Diga la Piastra	11	371300.62	4898311.57
Diga del Chiotas	12	366804.91	4891116.38
Valdieri	13	361620.97	4896069.5
Colle Lombarda	14	352018.38	4896619.03
Vinadio Stura di Demonte	15	349618.72	4907200.09
San Giacomo Demonte	16	356770.16	4911824.79
Demonte	17	365404.39	4908399.72
Monterosso Grana	18	366590.31	4918715.35
Dronero	19	373559.3	4923237.86

Castiglione Saluzzo	20	380539.79	4934927.61
Fossano	21	403650.7	4932444.27
Palanfrè	22	379219.4	4894456.54
Limone Pancani	23	387343.41	4890811.23
Rifugio Mondovì	24	398684.41	4893942.97
Upega	25	398022.64	4887039.55
Piaggia	26	398412.55	4880615.44

# 6.3 Assessment of the Temporal Lag between Precipitation and Water Table Levels

To identify the lag between rainfall events and groundwater responses, daily precipitation data for the basin and piezometric levels from ARPA (piezometer T03 for the Beinette Basin, and piezometer T02 for the Tetti Pesio Basin) were analysed.

Precipitation data were smoothed with a 60-day moving average to reduce short-term peaks, as groundwater response is typically attenuated and delayed. The smoothed precipitation curve was then progressively shifted until it showed a comparable trend to the groundwater level curve.

# 6.4 Assessment of the MAR Influence on the Underlying Aquifer

Finally, the influence of MAR infiltrations on the water table was assessed. Piezometric data from six monitoring wells were analysed. The main objective was to identify possible anomalies in the piezometer located downstream of the infiltration trench, in order to verify whether the water table dynamics were influenced by artificial recharge rather than by natural precipitation patterns. As in the previous analysis, MAR infiltration data were smoothed using a 20-days moving averaged to account for damping effect of groundwater dynamics on infiltration, and a temporal delay was applied according to the results obtained in the phase described in the previous section.

## 7 RESULTS

This chapter presents the results obtained for the Beinette and Tetti Pesio MAR systems.

First of all, it analyses the relationship between the water level in the channels and the corresponding flowrate, which was used to calculate the water volumes infiltrated during the study.

Successively, it illustrates the precipitation study, through the application of Thiessen Polygons. Finally, it examines the temporal lag between the precipitation and the aquifer response, in order to study the real effects of the MAR infiltration on the groundwater table.

### 7.1 Beinette

### 7.1.1 Volume of water infiltrated

The rating curves in presented in Figure 24 were derived using the WinFlume software for the upstream and downstream weirs of the Beinette MAR system.

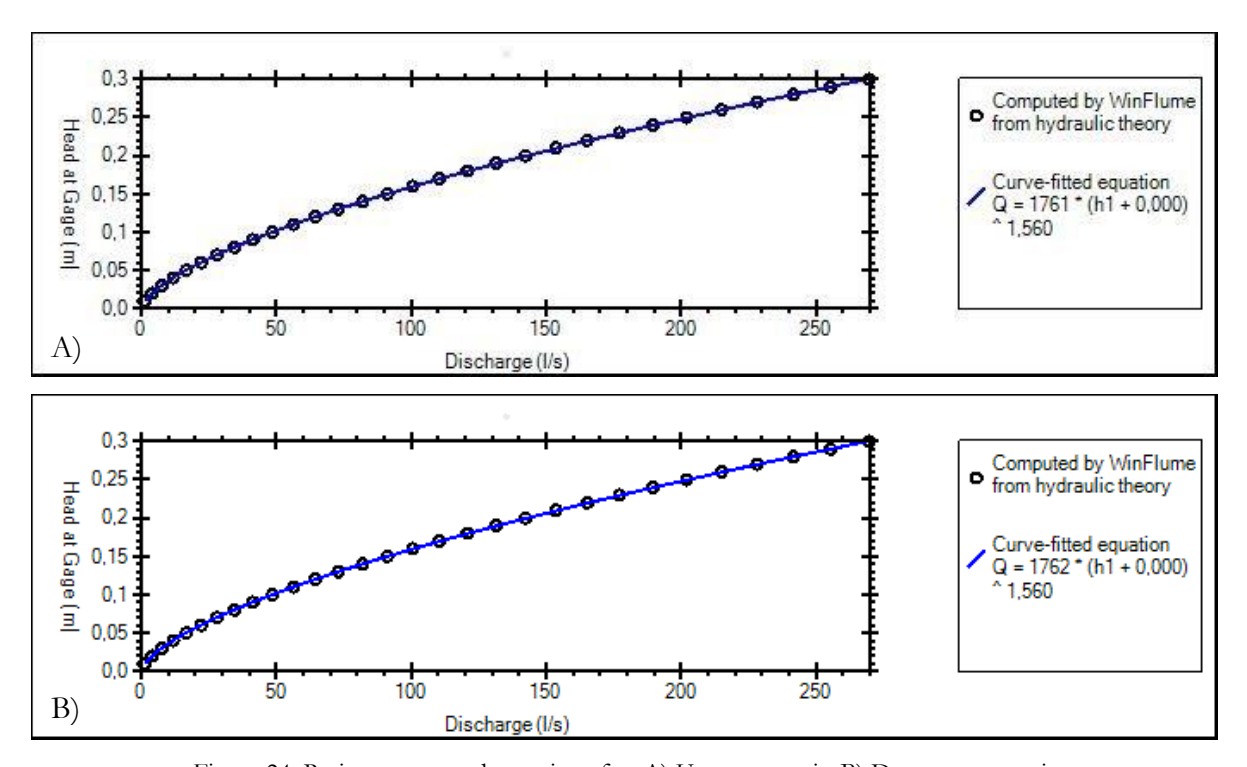


Figure 24. Rating curves and equations for: A) Upstream weir; B) Downstream weir

The rating curves follow a power-law trend, as expected from the theoretical behaviour of the broad-crested weir

The relationship between the water head and the corresponding flowrate was then used for the estimation of the volume of water infiltrated through the infrastructure over the study period.

In particular, the parameters from the curve-fitted equation (Table 8) were used for the correlations, using Equation 6, presented in Section 6.1.1.2.

Table 8. Parameters obtained through WinFlume for the head-flowrate correlation

Parameter	Upstream	Downstream
k	1761	1762
u	1.56	1.56

The discharge passing through the two weirs was estimated using the water level measured by two pressure dataloggers, which were then corrected with the application of the offsets.

The collected data are shown in Figure 25.

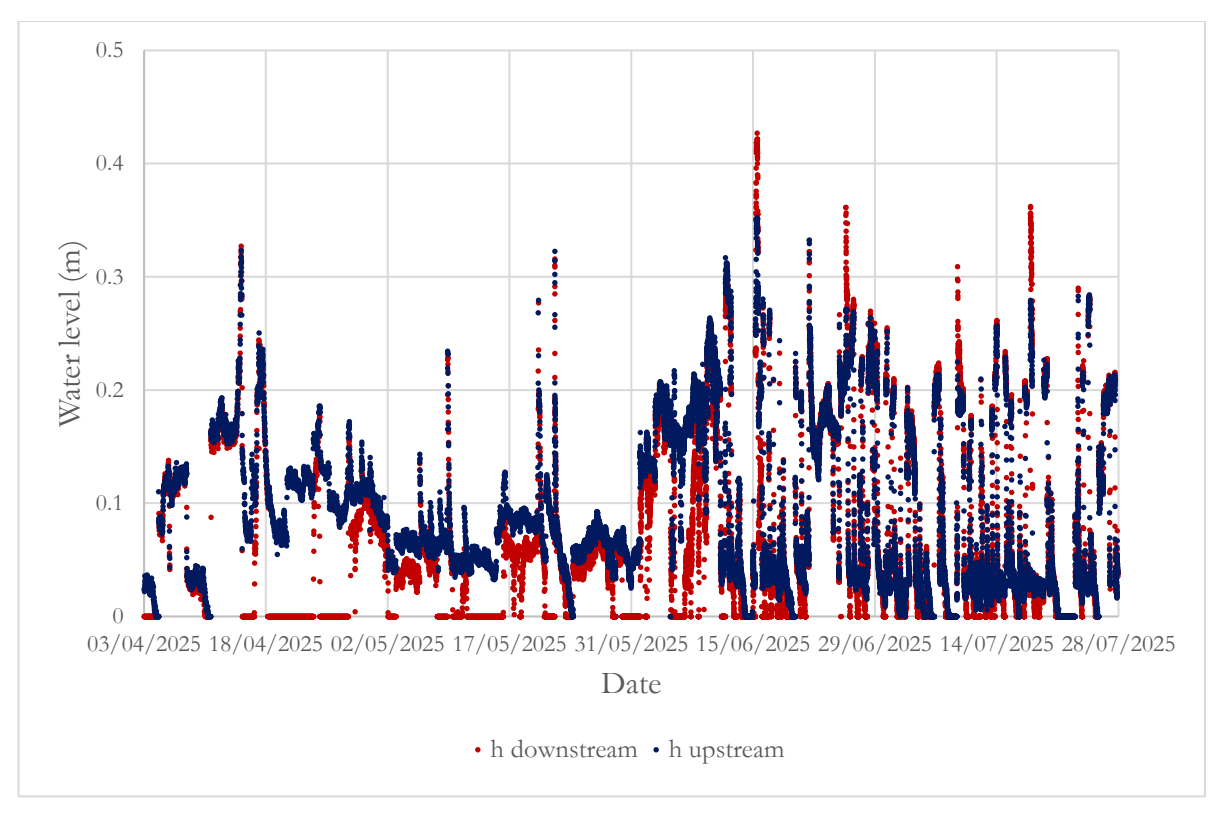


Figure 25. Water head measured over the upstream and downstream broad-crested weirs

As expected, since the two weirs are similar in geometry, the upstream water level (blue dots) is most of the time higher or equal to the downstream one (red dots).

When the red dots are placed on the x-axis, there is no discharge over the downstream weir, meaning that all the water coming from the channel is infiltrated into the underlying aquifer.

The daily infiltrated volume is shown in Figure 26, with the red line representing the cumulative volume.

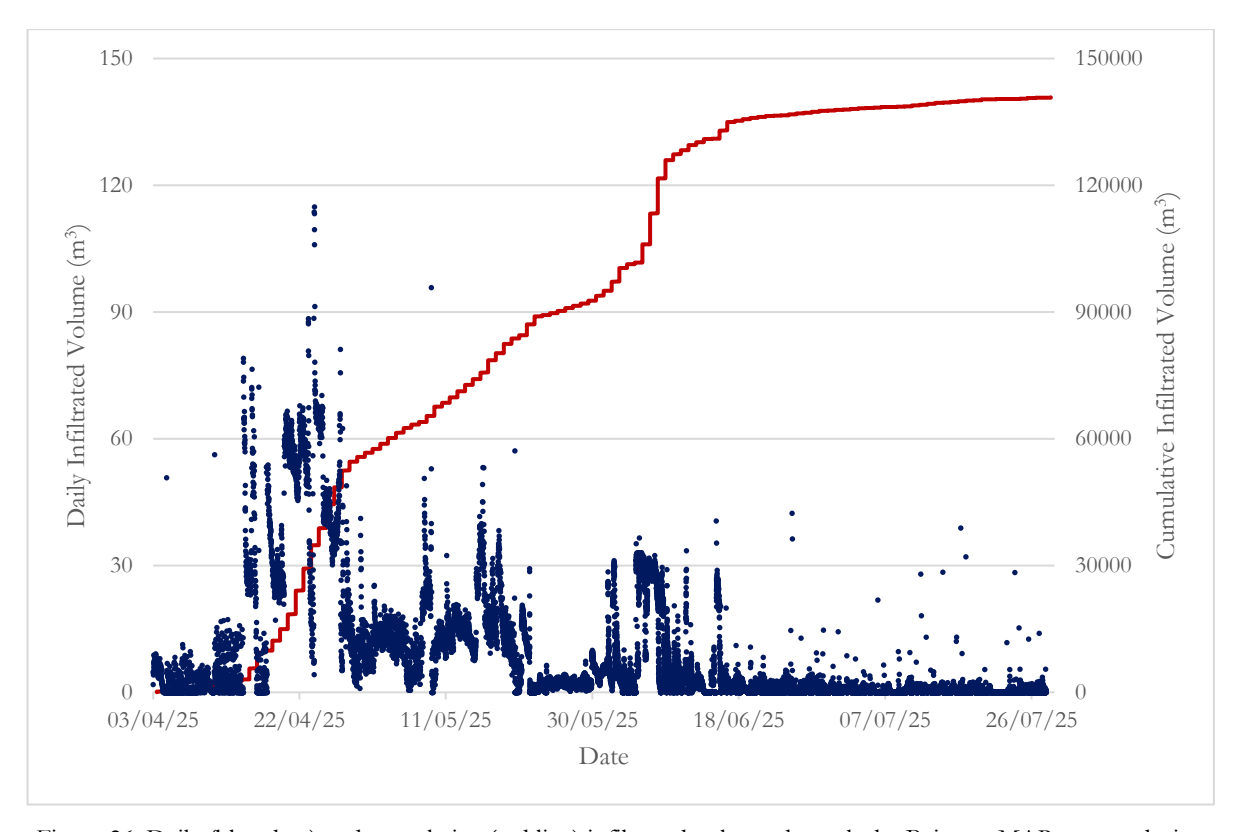


Figure 26. Daily (blue dots) and cumulative (red line) infiltrated volume through the Beinette MAR system during the study period

It was estimated that during the period 03/04/2025-28/07/2025 a total of  $140773.10 \, m^3$  of water was infiltrated through the Beinette MAR system, with an average flowrate of  $50.13 \, m^3 h^{-1}$ .

### 7.1.2 Precipitation study

The Beinette basin was delineated using specific QGIS tools applied to the Piedmont DEM (Figure 27).

Subsequently, additional QGIS functions were used on the basin map in order to identify the pluviometric stations defining the precipitation over it.

To this end, Thiessen Polygons were generated (Figure 28), and the areas of the intersections between the polygons and the basin were calculated.

From these, weighting factor was derived, expressed as the percentage of each intersection area with respect to the total basin area (Table 9).

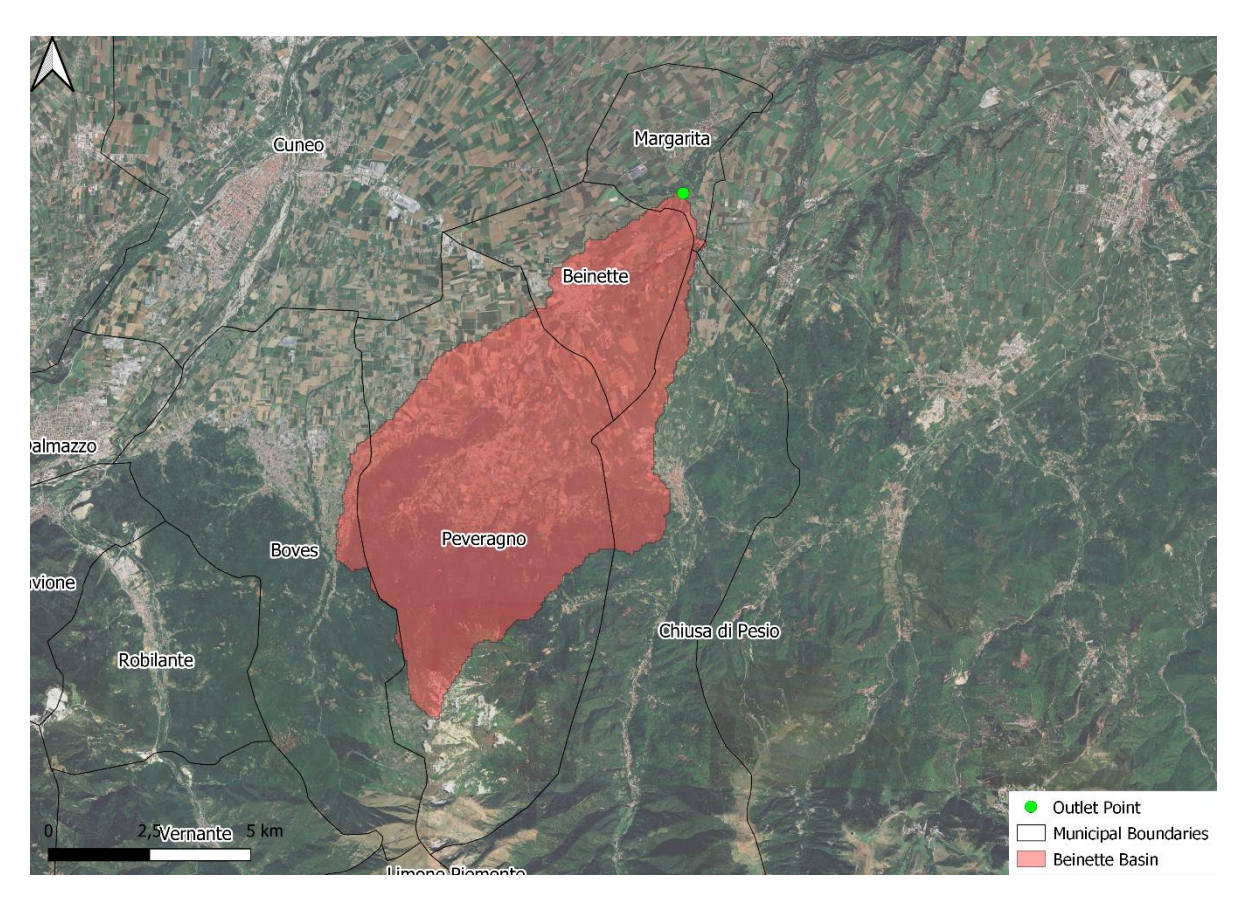


Figure 27. Beinette Basin delineated using QGIS

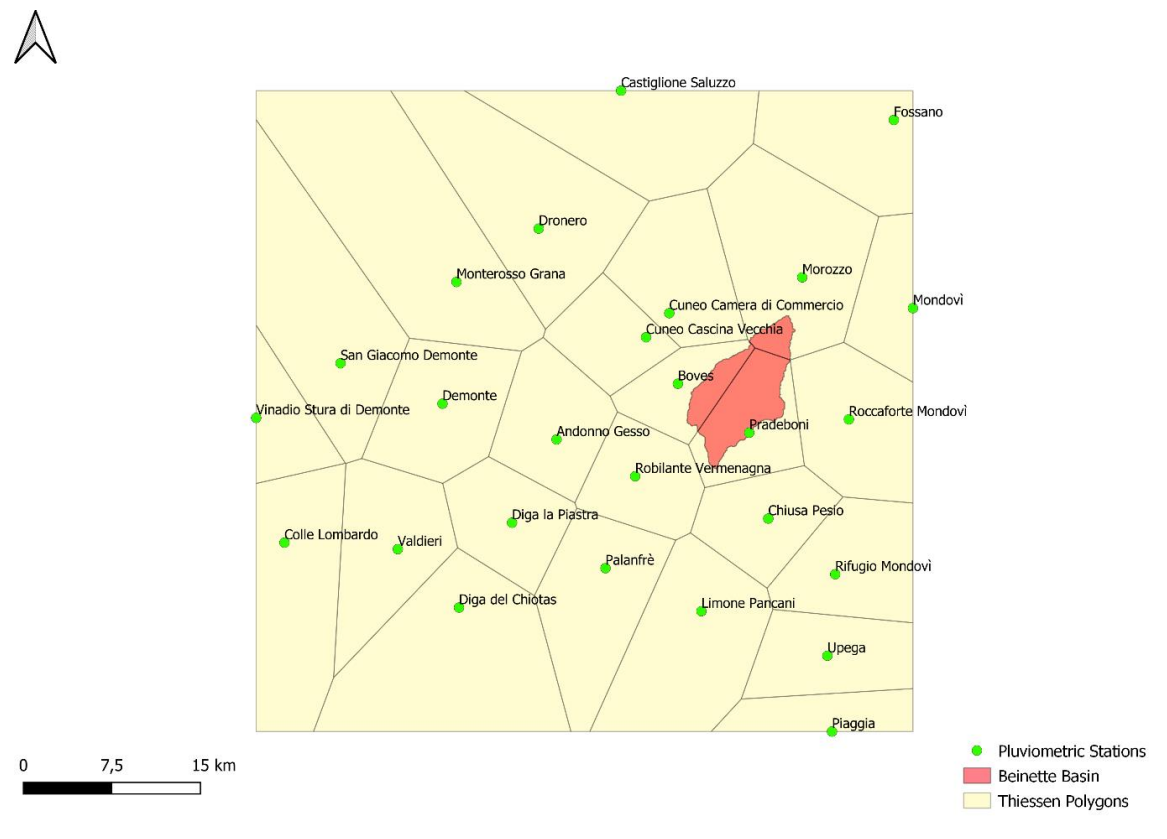


Figure 28. Thiessen Polygons built around Beinette Basin

Table 9. Area and corresponding percentage of the Thiessen Polygons and Beinette basin intersections

Pluviometric Station	Area (km²)	%
Boves	13758127.84	23.25
Morozzo	8047036.57	13.60
Pradeboni	37359835.57	63.15
Total	59164999.98	100

Using the weighting factor in Table 9, the mean height of precipitation over Beinette basin was calculated for the period 01/01/2021-08/09/2025, as shown in Figure 29.

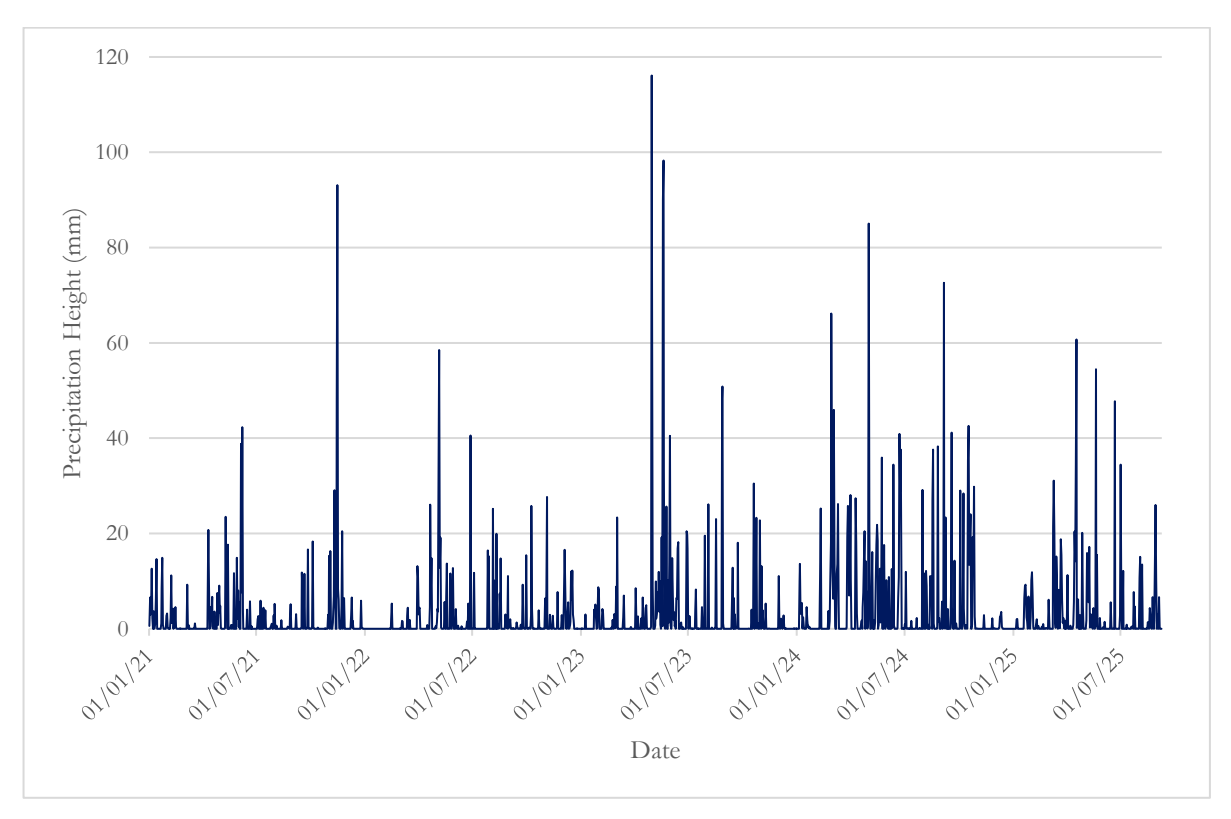


Figure 29. Daily precipitation over Beinette basin

Subsequently, Figure 30 shows the 60-day moving average of precipitation, plotted with a 10-day temporal lag relative to the groundwater level measured by ARPA.

The precipitation (blue) and groundwater level (red) curves follow similar trend, confirming that a 10-days temporal lag is appropriate.

This delay is evident during the two main rainy periods (from May 2023 to November 2023, and from April 2024 to January 2025). During these intervals, the two curves exhibit synchronous peaks and similar patterns, with both positive and negative trends showing a strong correlation.

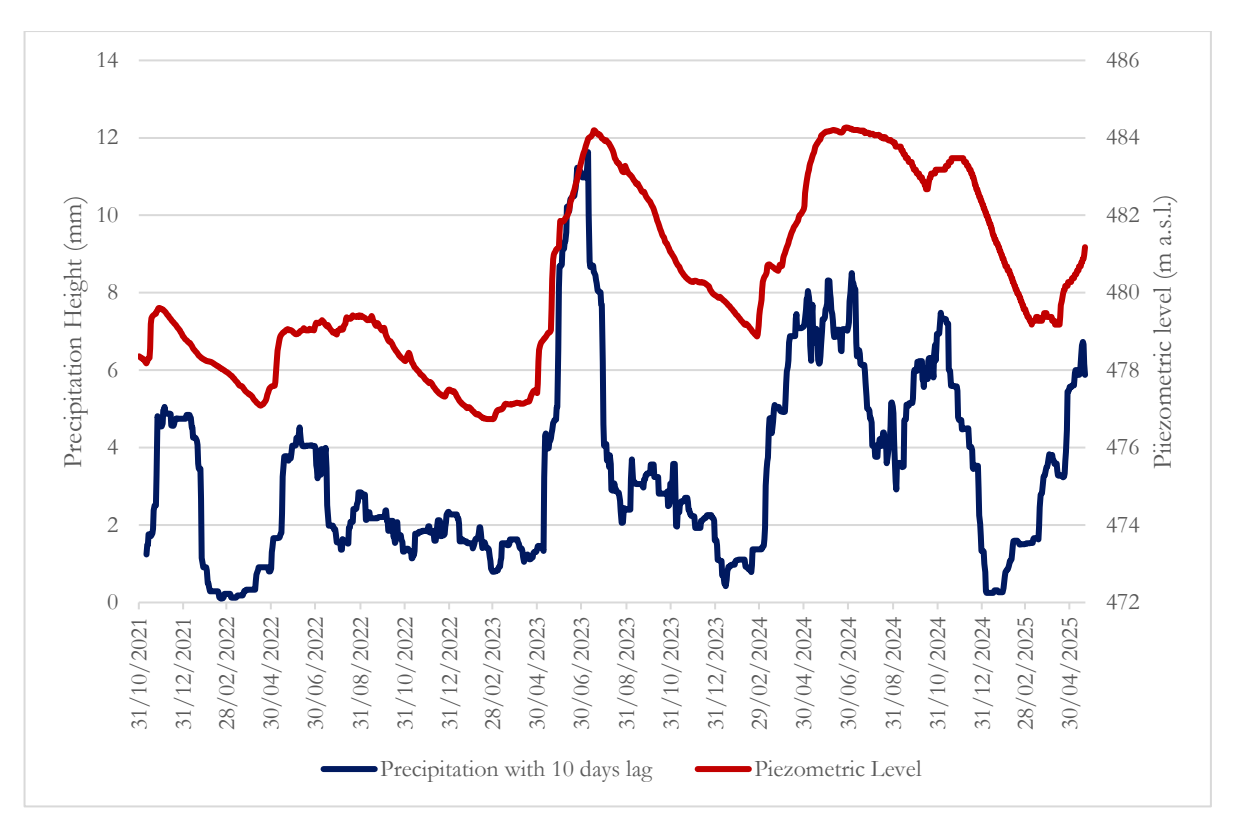


Figure 30. Shifted 60-day moving average of precipitation and groundwater level

This relationship is further highlighted by the scatter plot between groundwater level and precipitation shown in Figure 31.

The coefficient of determination ( $R^2$ =0.4693) indicates a moderate positive correlation between the two variables. The fact that  $R^2$  is somewhat lower than 1 (perfect correlation) can be explained by the aquifer recession phases, when the water table diminishes gradually, while precipitation shows an abrupt decrease, resulting in a weaker relationship.

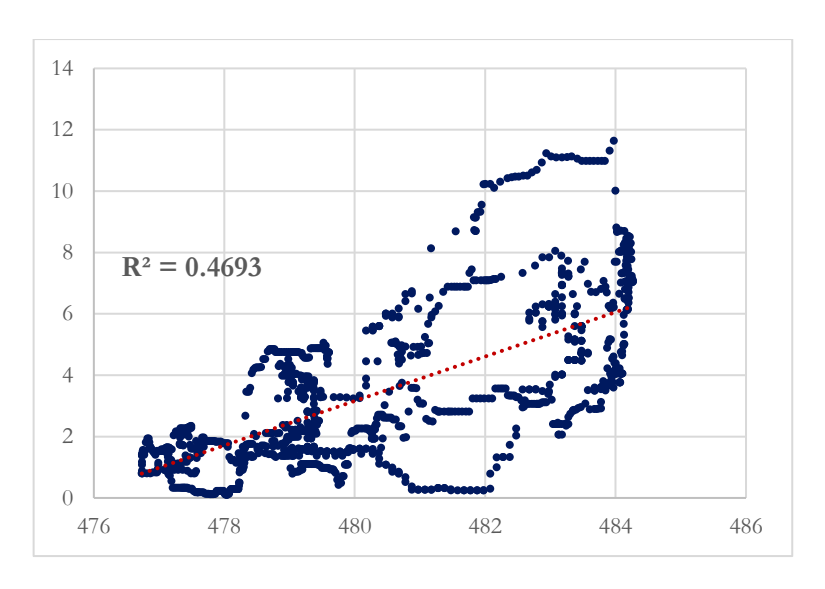


Figure 31. Scatter plot between groundwater level and precipitation

### 7.1.3 MAR infiltration and groundwater relation

All the results obtained in the previous passages, were finally combined to correlate precipitation, MAR infiltration, and groundwater levels.

As for the infiltration, a 20-day moving average was applied, and the data were shifted of 10 days, consistently with the previous results. The infiltration was then divided by 10, to make them comparable in scale with the other data in the graph.

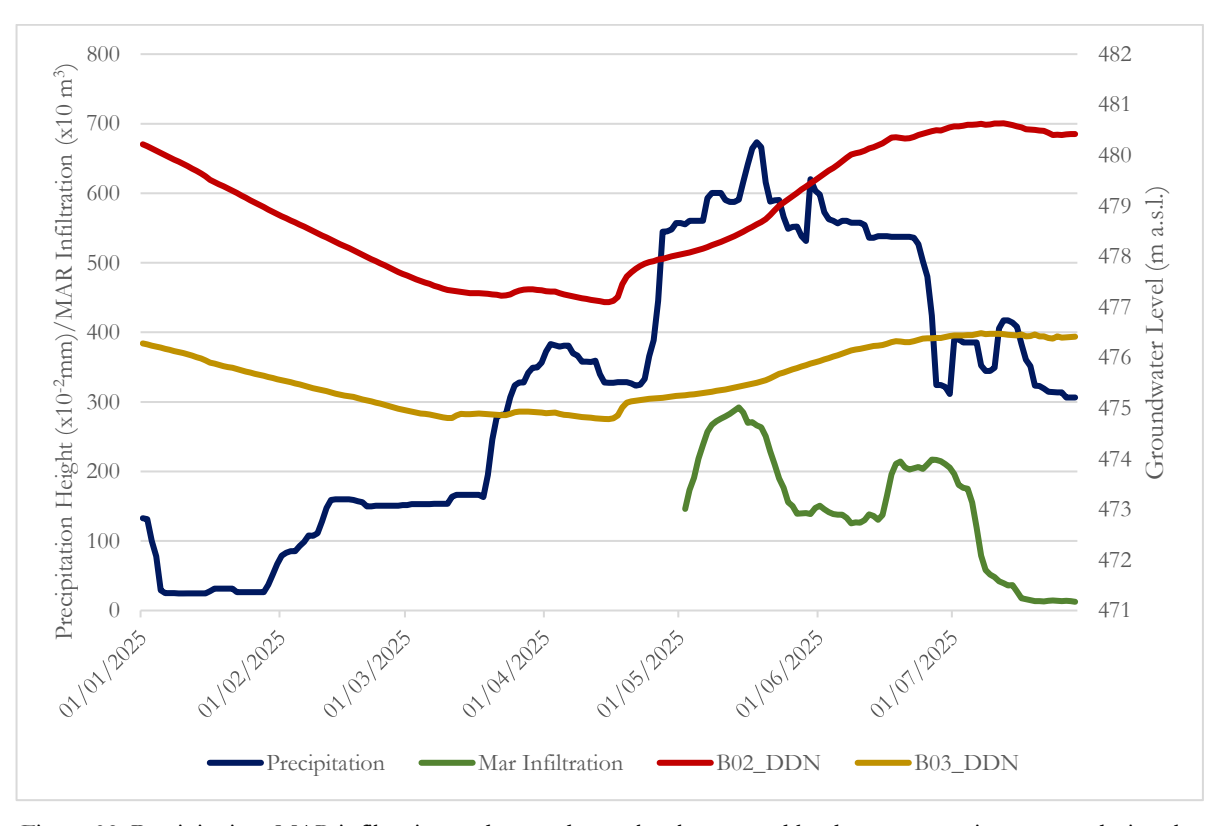


Figure 32. Precipitation, MAR infiltration and groundwater level measured by downstream piezometers during the study period

Figure 32 shows precipitation and Beinette MAR infiltration plotted against the groundwater level measured by the downstream piezometers B02\_DDN and B03\_DDN.

The groundwater level increases simultaneously with the beginning of MAR infiltration and continues the rise even after precipitation starts to decrease, however, the correlation is not completely clear.

Unfortunately, the available dataset is not sufficiently long to provide a complete evaluation of the MAR infiltration and groundwater level correlation.

The low reliability of this correlation is shown in Figure 33, which plots data from all the piezometers used in the study. In fact, groundwater level at all the locations continue to rise, even after the precipitation decreases, indicating that other factors may influence the system's response.

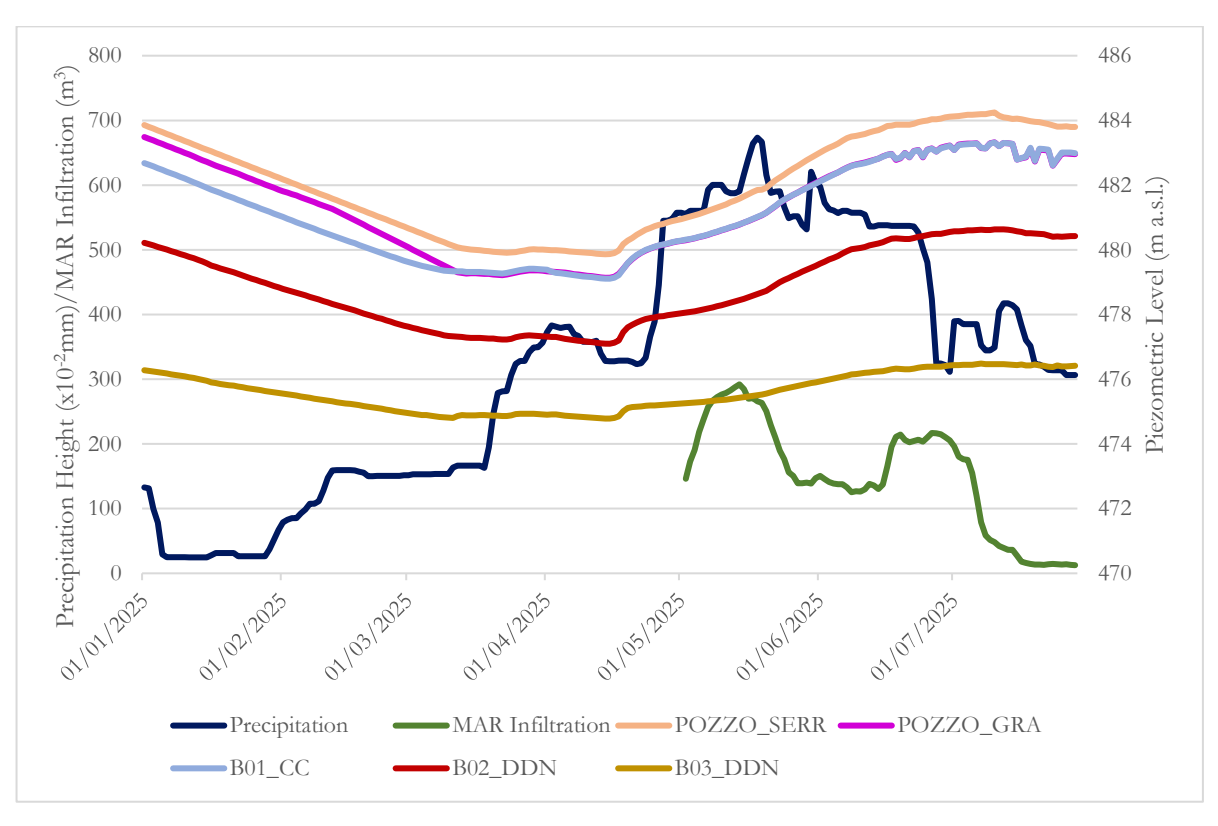


Figure 33. Precipitation, MAR infiltration and groundwater level measured by all the piezometers during the study period

### 7.2 Tetti Pesio

### 7.2.1 Volume of water infiltrated

The rating curves used to relate the water level at the upstream datalogger and the head over the sluice gate with the channel flowrate were obtain through four discharge measurements and are shown in Figure 34.

These curves were used to derive the equations that links the water levels to the flowrate, and to obtain the parameters required for Equation 13, described in Section 6.1.2.2 (Table 10).

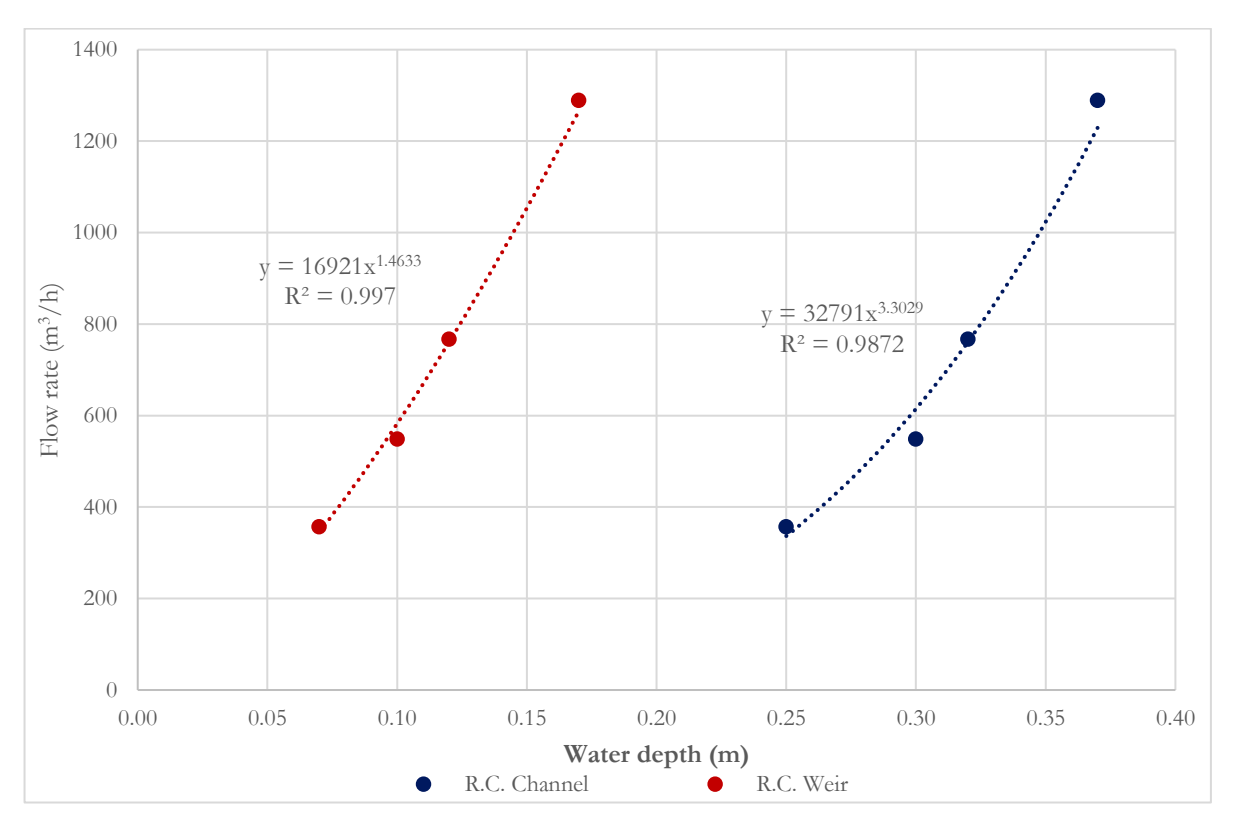


Figure 34. Rating curves obtained for the upstream datalogger and for the head over the sluice gate

Table 10. Parameters obtained through the rating curves for the head-flowrate correlation

Parameter	Upstream	Sluice Gate	
k	32791	16921	
u	1.4633	3.3029	

The discharges at the two points were calculated through the water head measured by dataloggers, shown in Figure 35.

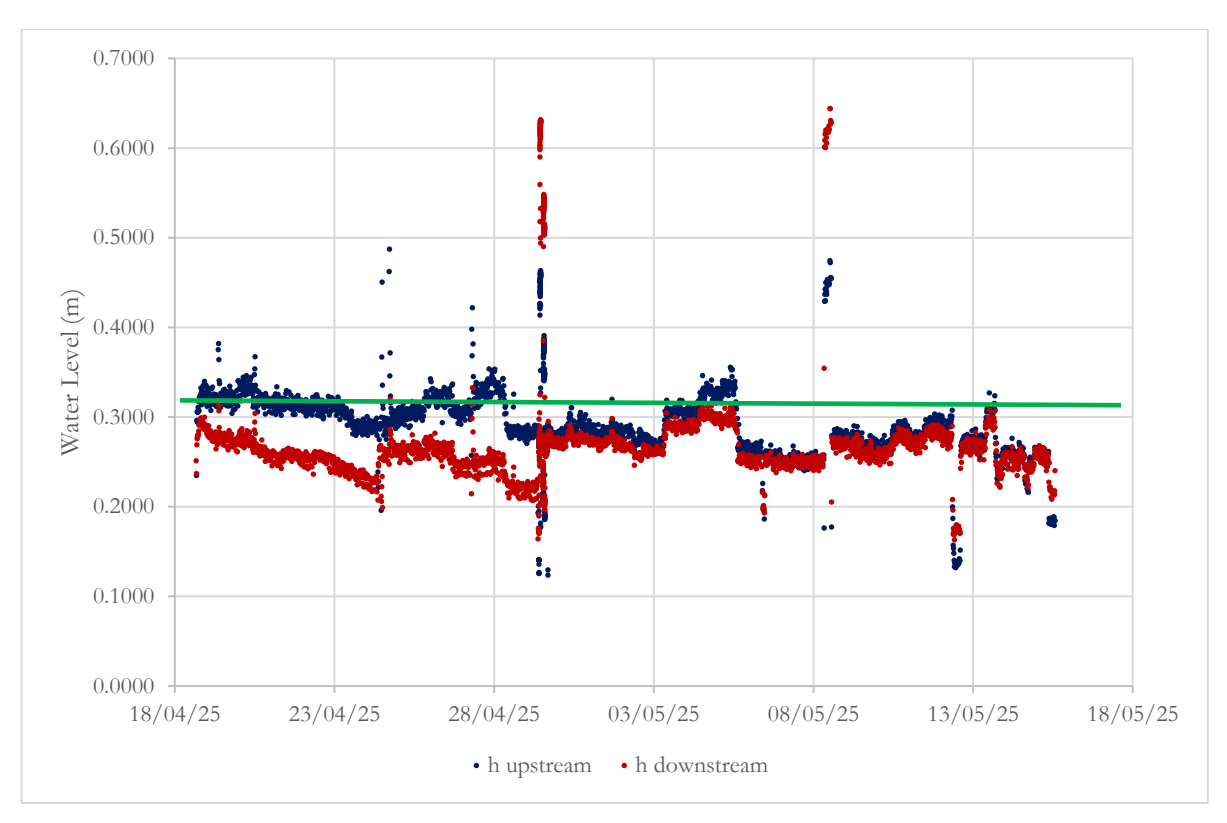


Figure 35. Water level measured by the two datalogger located in the channel with the green line representing the sluice gate height

The green line represents the sluice gate height (0.31m). During the study period, the downstream head level exceeded the gate height in two occasions, on 29/04/2025 and on 08/05/2025. This indicates that the sluice gate was placed in the channel only in these two days. Consequently, infiltration through the MAR infrastructure was active only during these two short events.

Because of this limited operation time, it was not possible to carry out meaningful analysis of the infiltrated volumes or their effect on the groundwater level. The infiltration events were too few and of short duration, lasting less than one day each, to generate measurable aquifer response. Therefore, this study focuses on establishing the monitoring setup that will enable a more comprehensive analysis in future campaigns, when more consistent infiltration will be available.

### 7.2.2 Precipitation study

The Tetti Pesio basin was delineated using specific QGIS tools applied to the Piedmont DEM (Figure 36).

As done for the Beinette basin, Thiessen Polygons were generated (Figure 37) applying additional QGIS functions to identify the pluviometric stations defining the precipitation over it. Finally, the areas of the intersections between the polygons and the basin were calculated.

From these, weighting factor was derived, expressed as the percentage of each intersection area with respect to the total basin area (Table 11).

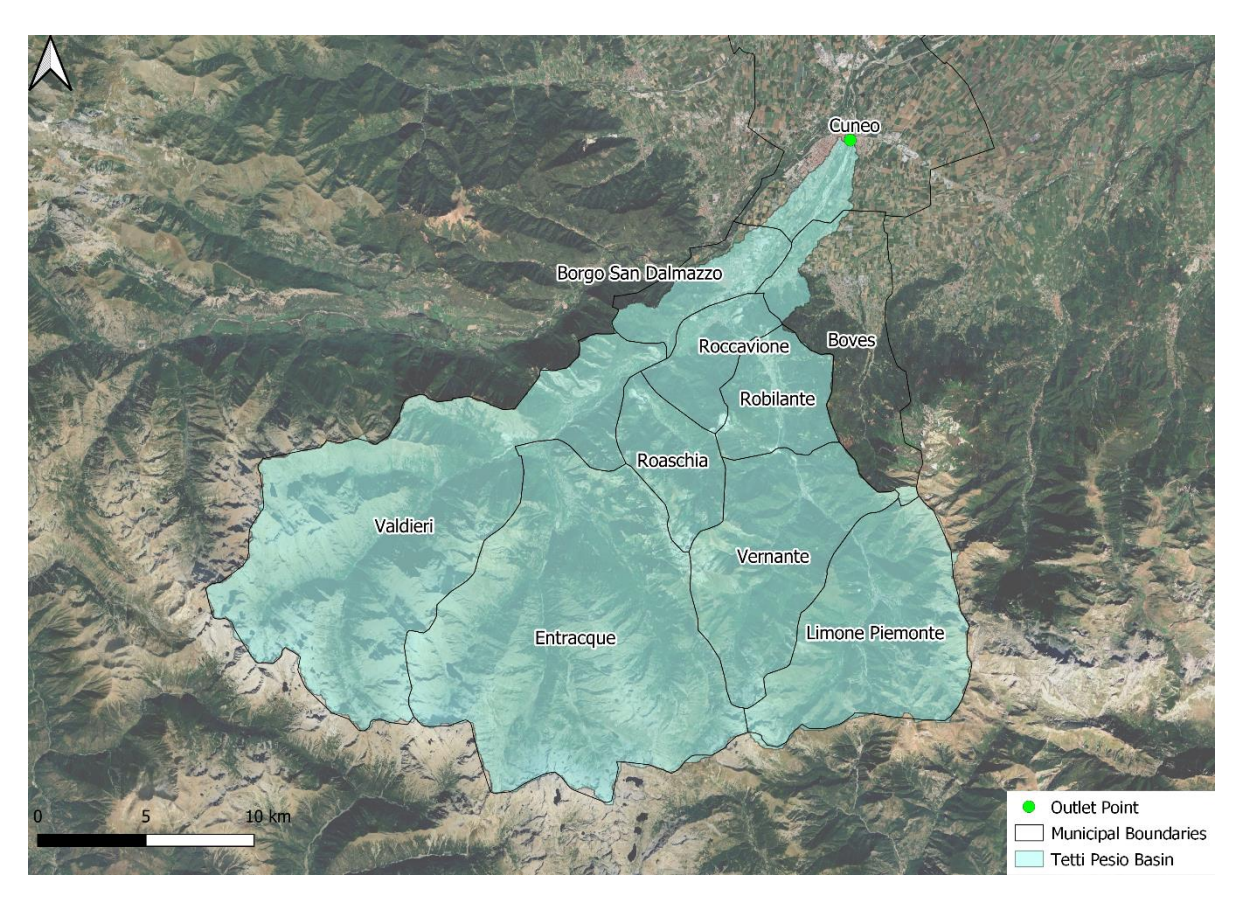


Figure 36. Tetti Pesio Basin delineated using QGIS





Diga del Chiotas

Rifugio Mondovì

Upega

Limone Pancani

Figure 37. Thiessen Polygons built around Tetti Pesio Basin

Table 11. Area and corresponding percentage of the Thiessen Polygons and Tetti Pesio basin intersections

Pluviometric Station	Area (km²)	0/0
Colle Lombarda	2541177	0.004616
Valdieri	84666427	0.153783
Diga del Chiotas	72800255	0.13223
Palanfrè	95281149	0.173063
Limone Pancani	48985769	0.088975
Demonte	8945493	0.016248
Diga la Piastra	79403315	0.144223
Chiusa Pesio	10348417	0.018796
Robilante Vermenagna	63457341	0.11526
Andonno Gesso	56364493	0.102377
Boves	9625580	0.017483
Cuneo Cascina Vecchia	15460842	0.028082
Cuneo Camera di Commercio	2677237	0.004863
Total	550557495	1

Using the weighting factors in Table 11, the mean precipitation over Tetti Pesio basin was calculated for the period 01/01/2021-11/10/2025, as shown in Figure 38.

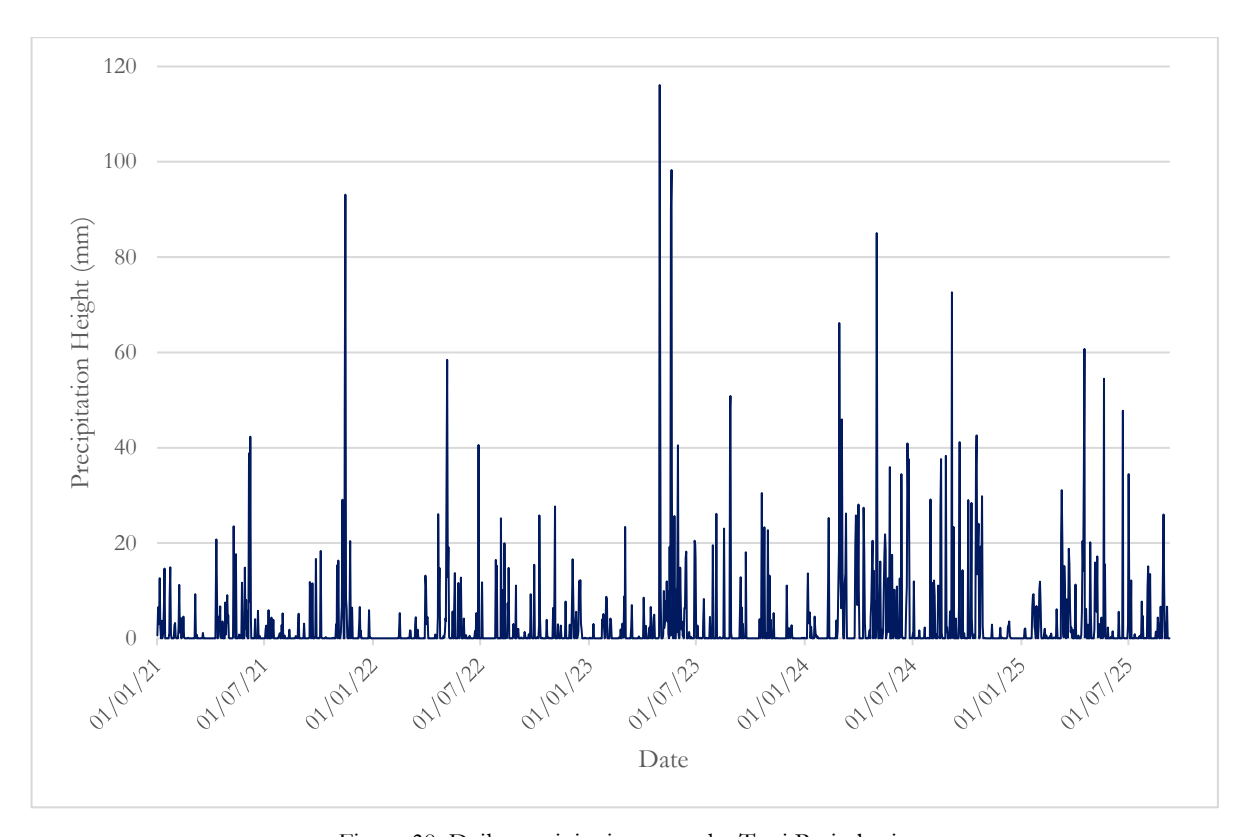


Figure 38. Daily precipitation over the Tetti Pesio basin

Subsequently, Figure 39 shows the 60-day moving average of precipitation, plotted with a 10-day temporal lag relative to the groundwater level measured by ARPA.

The precipitation (blue) and groundwater level (red) curves follow similar trend, confirming that a 10-days temporal lag is appropriate.

This delay is evident during the main rainy periods, when the two curves exhibit synchronous peaks and similar patterns, with both positive and negative trends showing a strong correlation. This relationship is further highlighted by the scatter plot between groundwater level and precipitation shown in Figure 40. As for Beinette basin, the coefficient of determination (R<sup>2</sup>=0.5638) indicates a moderate positive correlation between the two variables. Even in this case, this coefficient is somewhat lower than 1, and the explanation is in the different behaviour of the two curves during the recession phases.

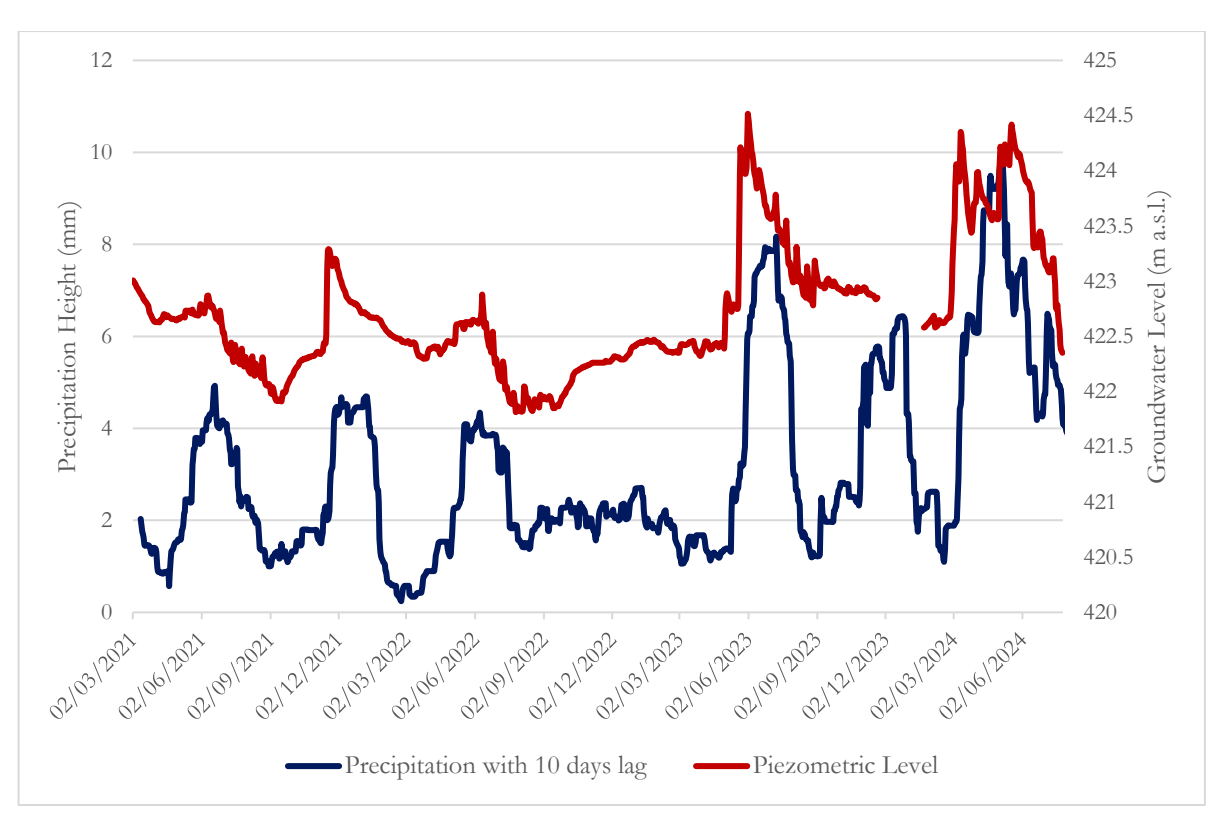


Figure 39. Shifted 60-day moving average of precipitation and groundwater level

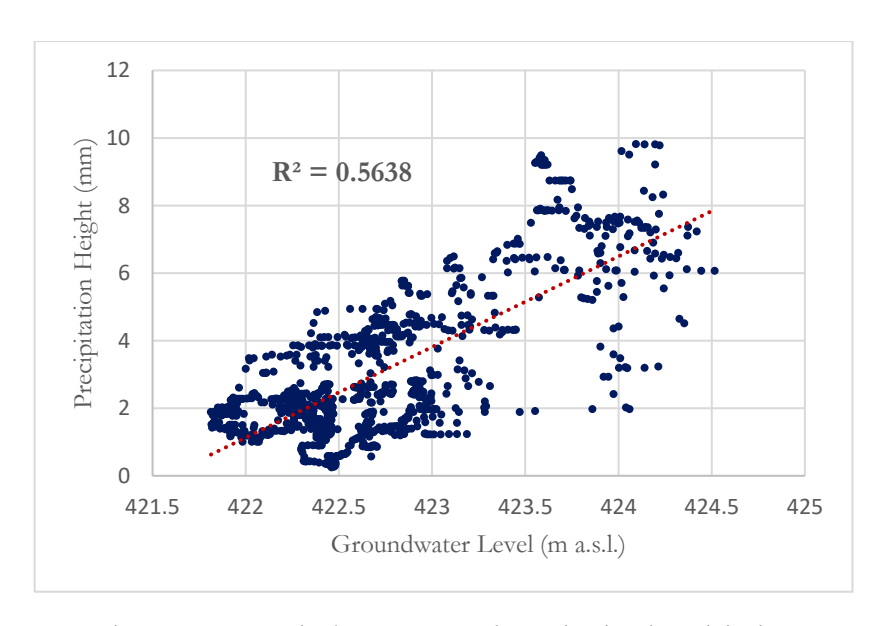


Figure 40. Scatter plot between groundwater level and precipitation

# 7.2.3 Groundwater levels

Finally, Figure 41 shows the groundwater levels registered by the piezometers used in the study.

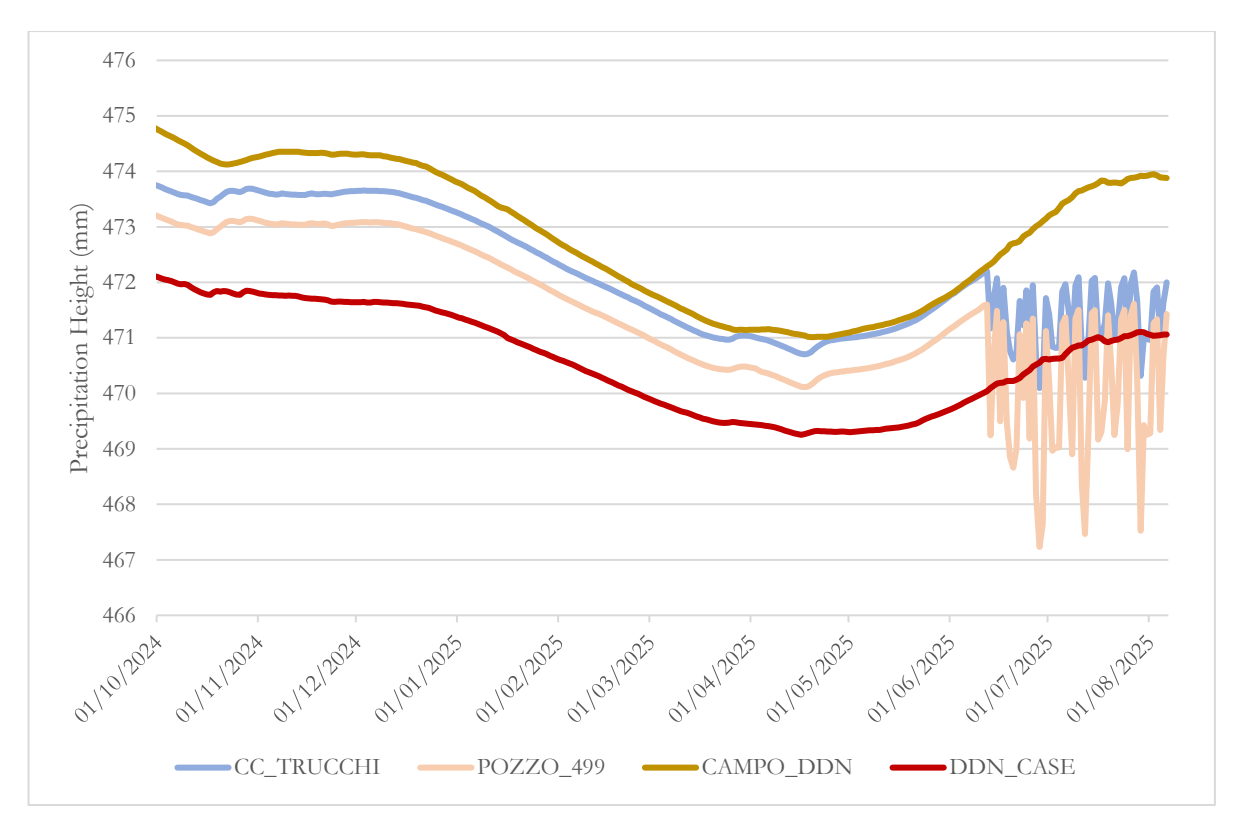


Figure 41. Groundwater levels measured by the piezometers in the Tetti Pesio MAR study

The groundwater level follows a similar trend across all the piezometers present in the zone. The piezometers give a comprehensive framework of the quantitative status of the aquifers, that it will be useful in the future to assess the effects of the MAR infiltrations on the underlying groundwater, once longer operational periods are achieved.

# 8 CONCLUSION

This study assessed the feasibility and the hydrological impact of two MAR infrastructures built in the Province of Cuneo, located in the municipalities of Beinette and Tetti Pesio, within the framework of the SeTe-Alcotra project. The objective of the study was to estimate the volume of infiltrated water through the MAR systems and to assess their influence on the underlying aquifer, isolating the effects of natural precipitation.

A combination of field monitoring data, spatial analysis with QGIS, and temporal correlation between hydrological variables was applied to estimate the infiltrated volume, delineate the basins, analyse the precipitation and monitor groundwater levels.

At the Beinette sites, during the monitoring period (April-July 2025), the study demonstrated an infiltration process capable to recharge a total volume of approximately 140,773  $m^3$  of water, with an average flowrate of 50.13  $m^3h^{-1}$ .

The precipitation study, carried out through the application of the Thiessen Polygons method, individuated 3 pluviometric stations representing rainfall over the Beinette basin, used to estimate the mean precipitation.

The temporal lag between precipitation and aquifer response was identified equal to 10 days.

Although MAR infiltration appeared to contribute to the rise in groundwater levels, the limited monitoring period did not allow for a clear quantification of the correlation between MAR infiltration and aquifer response.

At the Tetti Pesio site, during the monitoring period (April-May 2025), the infiltration process was possible only in two days (29 April and 8 May), and just for few hours. Due to these short durations, it was not possible to derive meaningful conclusions on the infiltration volume or its effects on the underlying aquifer.

However, the monitoring network provided a comprehensive framework of the quantitative status of the groundwater and sets a basis for future studies, when longer and more consistent infiltrations will be available.

The precipitation study for Tetti Pesio basin has individuated 13 pluviometric stations, used to calculate the mean precipitation over the basin. Similarly to Beinette, the temporal lag between precipitation and aquifer response was equal to 10 days.

In both recharge trenches, the coefficients of determination of the scatter plots between groundwater level and precipitations showed a moderate positive relationship (0.47 for Beinette, 0.56 for Tetti Pesio), due to the difference behaviour of the two variables during the recession phases.

The main limitation of this project lies in the short monitoring period and the limited operational activity of the MAR infrastructures.

Additionally, it was challenging to precisely isolate the precipitation effects from the MAR infiltration ones.

Further data acquisition over longer periods would allow to obtain more significant and relevant results, making it possible to evaluate the MAR system performance.

Future developments should focus on extending the monitoring period to better understand the influence of recharge on the aquifer. Moreover, monitoring during dry or low-precipitation periods would help to isolate the MAR effects from natural, providing a clearer scenario.

Overall, this study provides a valuable insight into the application of MAR systems in the Piedmont Region and confirm their potential as effective, natural-based solutions for groundwater resource enhancement.

Despite the limitations, the results highlight that, with adequate monitoring and operational continuity, MAR can play a strategic role in increasing aquifer resilience against water scarcity derived from climate change and in supporting sustainable water management in Northern Italy.

# 9 REFERENCES

- [1] O. Adedeji, O. Reuben, and O. Olatoye, 'Global Climate Change', *GEP*, vol. 02, no. 02, pp. 114–122, 2014, doi: 10.4236/gep.2014.22016.
- [2] 'What Is Climate Change? NASA Science'. Accessed: July 31, 2025. [Online]. Available: https://science.nasa.gov/climate-change/what-is-climate-change/
- [3] U. Nations, 'What Is Climate Change?', United Nations. Accessed: July 31, 2025. [Online]. Available: https://www.un.org/en/climatechange/what-is-climate-change
- [4] 'Copernicus: 2024 is the first year to exceed 1.5°C above pre-industrial level | Copernicus'. Accessed: Aug. 01, 2025. [Online]. Available: https://climate.copernicus.eu/copernicus-2024-first-year-exceed-15degc-above-pre-industrial-level
- [5] J. M. Last, K. Trouton, and D. Pengelly, *Taking our breath away: the health effects of air pollution and climate change.* Vancouver: David Suzuki Foundation, 1998.
- [6] 'Climate Change: Global Sea Level | NOAA Climate.gov'. Accessed: Aug. 01, 2025. [Online]. Available: https://www.climate.gov/news-features/understanding-climate/climate-change-global-sea-level
- [7] G. Chan, R. Stavins, and Z. Ji, 'International Climate Change Policy', *Annu. Rev. Resour. Econ.*, vol. 10, no. 1, pp. 335–360, Oct. 2018, doi: 10.1146/annurev-resource-100517-023321.
- [8] United Nations, 'UN Framework Convention on Climate Change (UNFCCC)'. Accessed: Aug. 01, 2025. [Online]. Available: https://unfccc.int/resource/docs/convkp/conveng.pdf
- [9] 'UN Framework Convention on Climate Change | EESC'. Accessed: Aug. 01, 2025. [Online]. Available: https://www.eesc.europa.eu/en/initiatives/un-framework-convention-climate-change
- [10] United Nations, 'Kyoto Protocol to the United Nations Framework Convention on Climate Change', Treaty FCCC/CP/1997/7/Add.1, 1998. Accessed: Aug. 01, 2025. [Online]. Available: https://unfccc.int/resource/docs/convkp/kpeng.pdf
- [11] United Nations, 'Paris Agreement', Treaty FCCC/CP/2015/10/Add.1, 2015. Accessed: Aug. 01, 2025. [Online]. Available: https://unfccc.int/sites/default/files/english\_paris\_agreement.pdf
- [12] C. Fetting, 'THE EUROPEAN GREEN DEAL'.
- [13] 'European Green Deal', Consilium. Accessed: Aug. 02, 2025. [Online]. Available: https://www.consilium.europa.eu/en/policies/european-green-deal/
- [14] 'Chapter 4: Future global climate: scenario-based projections and near-term information', in *Climate Change 2021: The Physical Science Basis*, in Sixth Assessment Report of the Intergovernmental Panel on Climate Change (AR6), Working Group I., Ginevra, Svizzera: Masson-Delmotte, V.; Zhai, P.; Pirani, A.; Connors, S. L.; Péan, C.; Berger, S.; Caud, N.; ... Zhou, B., 2021, pp. 553–672. Accessed: Aug. 04, 2025. [Online]. Available: https://www.ipcc.ch/report/ar6/wg1/downloads/report/IPCC\_AR6\_WGI\_Chapter04. pdf
- [15] N. Arnell, 'Climate change and global water resources', *Global Environmental Change*, vol. 9, pp. S31–S49, Oct. 1999, doi: 10.1016/S0959-3780(99)00017-5.
- [16] D. Page, E. Bekele, J. Vanderzalm, and J. Sidhu, 'Managed Aquifer Recharge (MAR) in Sustainable Urban Water Management', *Water*, vol. 10, no. 3, p. 239, Feb. 2018, doi: 10.3390/w10030239.
- [17] J. Ringleb, J. Sallwey, and C. Stefan, 'Assessment of Managed Aquifer Recharge through Modeling—A Review', *Water*, vol. 8, no. 12, p. 579, Dec. 2016, doi: 10.3390/w8120579.
- [18] H. Zhang, Y. Xu, and T. Kanyerere, 'A review of the managed aquifer recharge: Historical development, current situation and perspectives', *Physics and Chemistry of the Earth, Parts A/B/C*, vol. 118–119, p. 102887, Oct. 2020, doi: 10.1016/j.pce.2020.102887.

- [19] H. Bouwer, 'Artificial recharge of groundwater: hydrogeology and engineering', *Hydrogeology Journal*, vol. 10, no. 1, pp. 121–142, Feb. 2002, doi: 10.1007/s10040-001-0182-4.
- [20] P. Dillon, 'Future management of aquifer recharge', *Hydrogeol J*, vol. 13, no. 1, pp. 313–316, Mar. 2005, doi: 10.1007/s10040-004-0413-6.
- [21] P. Dillon *et al.*, 'Sixty years of global progress in managed aquifer recharge', *Hydrogeol J*, vol. 27, no. 1, pp. 1–30, Feb. 2019, doi: 10.1007/s10040-018-1841-z.
- [22] 'Maximize natural storage capacity INOWAS'. Accessed: July 24, 2025. [Online]. Available: https://www.inowas.com/applications/maximize-natural-storage-capacity/
- [23] 'Sustainable management of groundwater resources INOWAS'. Accessed: July 24, 2025. [Online]. Available: https://www.inowas.com/applications/a01-sustainable-management-of-groundwater-resources/
- [24] 'Assessment of saltwater intrusion INOWAS'. Accessed: July 24, 2025. [Online]. Available: https://www.inowas.com/applications/a07-assessment-of-saltwater-intrusion/
- [25] 'Assessment of water quality changes INOWAS'. Accessed: July 24, 2025. [Online]. Available: https://www.inowas.com/applications/assessment-of-water-quality-changes/
- [26] 'Sustain environmental surface water flows INOWAS'. Accessed: July 24, 2025. [Online]. Available: https://www.inowas.com/applications/sustain-environmental-surface-water-flows/
- [27] C. Seidl, D. Page, and S. A. Wheeler, 'Using managed aquifer recharge to address land subsidence: Insights from a global literature review', *Water Security*, vol. 23, p. 100184, Dec. 2024, doi: 10.1016/j.wasec.2024.100184.
- [28] 'Managed aquifer recharge INOWAS'. Accessed: July 13, 2025. [Online]. Available: https://www.inowas.com/mar/
- [29] P. Colombo, P. Mazzon, and L. Alberti, 'Off-season irrigation as a climate adaptation strategy for future groundwater management in Northern Italy', *Adv. Geosci.*, vol. 64, pp. 27–31, Aug. 2024, doi: 10.5194/adgeo-64-27-2024.
- [30] 'Aquifer storage and recovery (ASR) INOWAS'. Accessed: July 13, 2025. [Online]. Available: https://www.inowas.com/mar-methods/aquifer-storage-and-recovery-asr/
- [31] 'Aquifer storage, transfer, and recovery (ASTR) INOWAS'. Accessed: Aug. 06, 2025. [Online]. Available: https://www.inowas.com/mar-methods/aquifer-storage-transfer-and-recovery-astr/
- [32] 'Infiltration ponds and basins INOWAS'. Accessed: July 13, 2025. [Online]. Available: https://www.inowas.com/mar-methods/infiltration-ponds-and-basins/
- [33] 'Soil aquifer treatment (SAT) INOWAS'. Accessed: July 13, 2025. [Online]. Available: https://www.inowas.com/mar-methods/soil-aquifer-treatment-sat/
- [34] 'Induced bank filtration INOWAS'. Accessed: July 13, 2025. [Online]. Available: https://www.inowas.com/mar-methods/induced-bank-filtration/
- [35] 'Dune filtration INOWAS'. Accessed: Aug. 06, 2025. [Online]. Available: https://www.inowas.com/mar-methods/dune-filtration/
- [36] 'Subsurface dams INOWAS'. Accessed: July 14, 2025. [Online]. Available: https://www.inowas.com/mar-methods/subsurface-dams/
- [37] 'Sand dams INOWAS'. Accessed: July 14, 2025. [Online]. Available: https://www.inowas.com/mar-methods/sand-dams/
- [38] 'Rooftop rainwater harvesting INOWAS'. Accessed: July 14, 2025. [Online]. Available: https://www.inowas.com/mar-methods/rooftop-rainwater-harvesting/
- [39] Y. Zheng, A. Ross, K. G. Villholth, and P. Dillon, Eds, MANAGING AQUIFER RECHARGE: A Showcase for Resilience and Sustainability. UNESCO, 2021.
- [40] 'THE 17 GOALS | Sustainable Development'. Accessed: Aug. 27, 2025. [Online]. Available: https://sdgs.un.org/goals

- [41] Martin, 'Water and Sanitation', United Nations Sustainable Development. Accessed: Aug. 27, 2025. [Online]. Available: https://www.un.org/sustainabledevelopment/water-and-sanitation/
- [42] 'Water and Sanitation | Department of Economic and Social Affairs'. Accessed: Aug. 27, 2025. [Online]. Available: https://sdgs.un.org/topics/water-and-sanitation
- [43] 'Directive 2000/60 EN Water Framework Directive EUR-Lex'. Accessed: Aug. 27, 2025. [Online]. Available: https://eur-lex.europa.eu/eli/dir/2000/60/oj/eng
- [44] 'Directive 2006/118 EN EUR-Lex'. Accessed: Aug. 27, 2025. [Online]. Available: https://eur-lex.europa.eu/eli/dir/2006/118/oj/eng
- [45] 'Gazzetta Ufficiale'. Accessed: Aug. 28, 2025. [Online]. Available: https://www.gazzettaufficiale.it/dettaglio/codici/materiaAmbientale
- [46] 'Gazzetta Ufficiale'. Accessed: Aug. 28, 2025. [Online]. Available: https://www.gazzettaufficiale.it/eli/id/2016/06/13/16G00111/sg
- [47] 'Gazzetta Ufficiale'. Accessed: Aug. 28, 2025. [Online]. Available: https://www.gazzettaufficiale.it/eli/id/2023/04/14/23G00047/SG
- [48] 'Gazzetta Ufficiale'. Accessed: Aug. 28, 2025. [Online]. Available: https://www.gazzettaufficiale.it/eli/id/2023/06/13/23G00079/sg
- [49] 'Home | Alcotra 2021 2027'. Accessed: Sept. 17, 2025. [Online]. Available: https://www.interreg-alcotra.eu/it
- [50] 'SeTe ALCOTRA project', Groundwater Engineering Research Group. Accessed: Sept. 17, 2025. [Online]. Available: https://areeweb.polito.it/ricerca/groundwater/it/research/managed-aquifer-recharge-mar/sete-alcotra-project/
- [51] 'SeTe: Siccità e Territorio | Alcotra 2021 2027'. Accessed: Sept. 17, 2025. [Online]. Available: https://www.interreg-alcotra.eu/it/sete-siccita-e-territorio
- [52] Carraro, F. et al., 'Dati preliminari sulla neotettonica dei Fogli 56 (Torino), 68 (Carmagnola) e 80 (Cuneo)', C.N.R., Progetto Finalizzato Geodinamica, Sottoprogetto Neotettonica, Pubblicazione n. 155 del Progetto Finalizzato Geodinamica, 1978.
- [53] Alessandro Casasso, Elena Secco, and Maria Adele Taramasso, 'Siti sperimentali di ricarica controllata della falda in Provincia di Cuneo (CN)', Politecnico di Torino.
- [54] Alessandro Casasso *et al.*, 'INTERREG ALCOTRA 2021-2027 Progetto "SeTe: Siccità e Territorio" Relazione attività 1° anno (ottobre 2023 settembre 2024)', Politecnico di Torino, Torino, Dec. 2024.
- [55] A. Gaffar, 'Development of Pakistan's New Area Weighted Rainfall Using Thiessen Polygon Method', vol. 9, no. 17.
- [56] I. Yamada, 'Thiessen Polygons', in *International Encyclopedia of Geography*, John Wiley & Sons, Ltd, 2016, pp. 1–6. doi: 10.1002/9781118786352.wbieg0157.